DEPARTMENT OF ELECTRICAL AND COMPUTER ENGINEERING
COLLEGE OF ENGINEERING AND TECHNOLOGY
OLD DOMINION UNIVERSITY
NORFOLK, VIRGINIA 23529

GUIDANCE AND CONTROL STRATEGIES FOR AEROSPACE VEHICLES

By

Joseph L. Hibey, Principal Investigator

and

Desineni S. Naidu, Co-Principal Investigator

Final Report
For the period ended July 31, 1990

Prepared for
National Aeronautics and Space Administration
Langley Research Center
Hampton, Virginia 23665

Under
Research Grant NAG-1-736
Dr. Daniel D. Moerder, Technical Monitor
GCD-Spacecraft Controls Branch

Submitted by the
Old Dominion University Research Foundation
P.O. Box 6369
Norfolk, Virginia 23508-0369

August 1990

GUIDANCE AND CONTROL STRATEGIES FOR AEROSPACE VEHICLES

(NASA Langley Grant NAG1-736)

PART I

This final report under NASA Langley grant NAG1-736 consists of two parts. Part I consists of the summary of the earlier work whose reports have been submitted at various times during the period (1/1/87 to 12/31/1989). Part II describes in detail the research work done during the period 1/1/1990 to 7/31/1990.

TABLE OF CONTENTS

	Page
I. INTRODUCTION	3
II. SUMMARY/ABSTRACT	7
III. LIST OF PUBLICATIONS	21

I. INTRODUCTION

The first part of the report concerns broadly the summary of the work done in the areas of singular perturbations and time scales (SPaTS), aerobraking technology, guidance and aerocruise.

(i) SPaTS

The dynamics of many control systems is described by high-order differential equations containing parameters such as small time constants, masses, moments of inertia, inductances, and capacitances. The presence of these "parasitic" parameters is often the source for the increased order and the "stiffness" of the system. The "curse" of the dimensionality coupled with the stiffness poses formidable computational complexities for the analysis and control of such large systems. Singularly perturbed systems are those whose order is reduced when the parasitic parameter is neglected. The methodology of singular perturbations and time scales (SPaTS) is a "boon" to control engineers in tackling these large scale systems. As such it is very desirable to formulate many control problems to fit into the framework of the mathematical theory of SPaTS.

The methodology of SPaTS has an impressive record of applications in a wide spectrum of fields including flight mechanics and trajectory optimization. The aerospace problems involve, in general, the solution of nonlinear differential equations by resorting to numerical integration. Analytical solutions are important in providing a general understanding of the structure of solutions and a better foundation for the solution of guidance problems. With this in view, attempts have been made to obtain approximate analytical solutions for the atmospheric entry problem using asymptotic methods such as the method of matched asymptotic expansions, singular perturbation method, and multiple scale method.

In this report, using the theory of SPaTS, the various types of aerospace-related problems investigated were digital flight control systems [1-3, 6-8, 10, 14, 16]* and atmospheric entry problems [9-11, 18, 21, 22].

* *The numbers in brackets indicate the item under List of Publications.*

(ii) Aerobraking Technology

The specification spectrum for the proposed Space Transportation System (STS) places heavy emphasis on the development of reusable avionics subsystems having special features such as vehicle evaluation and reduction of ground support for mission planning, contingency response and verification and validation. According to the report of the National Commission on Space, **PIONEERING THE SPACE FRONTIER**, the concept of aerobraking for orbit transfer has been recognized as one of the critical technologies and recommended for demonstration projects in building the necessary technology base for pioneering the space frontier. In space transportation systems, the aerobraking, defined as the deceleration resulting from the effects of atmospheric drag upon a vehicle during orbital operations, opens new mission opportunities, especially with regard to the initiation of a permanent space station.

The main function of space transportation system is to deliver payloads from Earth to various locations in space. Until now, this function has been performed by various rockets, the space shuttle, and expendable upper stages using solid or liquid propellants. In particular, considering the economic benefits and reusability, an orbital transfer vehicle (OTV) is proposed for transporting payloads between low Earth orbit (LEO) and high Earth orbit (HEO). The two basic operating modes contemplated for OTV are a ground-based OTV which returns to Earth after each mission and a space-based OTV which operates out of an orbiting hanger located at the proposed Space Station Freedom.

In a typical mission, a space-based OTV, which is initially at the space station orbit (SSO), is required to transfer a payload to geosynchronous Earth orbit (GEO), pick up another payload, say a faulty satellite, and return to mate with the orbiting hanger at SSO for refurbishment and redeployment of the payload. The OTV on its return journey from GEO to SSO needs to dissipate some of its orbital energy. This can be accomplished by using an entirely propulsive (Hohmann) transfer in space only or a combination of propulsive transfer in space and aerobraking maneuver in the atmosphere. It has been established that a significant fuel savings and hence increased payload capabilities can be achieved with propulsive and aerobraking (or aeroassisted)

maneuvers instead of all-propulsive maneuvers. The word "aeroassisted" is often used to convey that the atmosphere is used to achieve the desired deceleration. This leads to an aeroassisted orbital transfer vehicle (AOTV), which on its return leg of the mission, dips into the Earth's atmosphere, utilizes atmospheric drag to reduce the orbital velocity and employs lift and bank angle modulations to achieve a desired orbital inclination. Basically, the AOTV performs a synergetic maneuver, employing a hybrid combination of propulsive maneuver in space and aerodynamic maneuver in the atmosphere. Broadly speaking, the two kinds of orbital transfer are coplanar orbital transfer and noncoplanar orbital transfer (or orbital transfer with plane change).

In this report, using algorithms based on industry standard program to optimize simulated trajectories (POST), and multiple shooting method, investigations have been carried out to generate fuel-optimal trajectories for coplanar orbital transfer [4, 12, 17, 25], and noncoplanar orbital transfer [13, 15, 19, 20, 29] arising in aerobraking technology.

(iii) Guidance

An optimal trajectory is computed for a given nonlinear dynamical system with a fixed set of conditions. However, variation of the initial and final conditions, plant parameters would alter the optimal trajectory. It is computationally tedious and expensive to repeat the whole optimization procedure for every changed condition and obtain a new optimal trajectory. In such a situation, an alternative is to linearize the original system and generate an optimal trajectory in the neighborhood of the original optimal trajectory, involving considerably less computational effort.

Guidance is the determination of a strategy for following a nominal flight in the presence of off-nominal conditions, wind disturbances, and navigation uncertainties. In a typical guidance scheme, the final steering command is generated as the sum of two components, an open-loop actuating (control) signal yielding the desired vehicle trajectory in the absence of external disturbances, and a linear feedback regulating signal which reduces the system sensitivity to unwanted influences on the vehicle.

In this report, guidance schemes for atmospheric maneuver for both deterministic and stochastic cases have been investigated [23, 24, 27].

(iv) Aerocruise

There are basically three methods of plane change, (i) impulsive method, (ii) aeroglide method, and (iii) aerocruise method. In impulsive method, the plane change is achieved entirely outside the atmosphere, and fuel consumption is prohibitively large for sizable changes of orbital plane. In both aeroglide and aerocruise methods, rockets are used to deflect the vehicle into the atmosphere, and the plane change is accomplished by heading change of the vehicle. With aeroglide there is no thrusting during the atmosphere, and with aerocruise, atmospheric drag is balanced by a continuous thrust to keep the spacecraft at a constant altitude and velocity. Propellent expenditure comparisons among the three methods of plane change show that the aerocruise method is superior to other competing methods for plane changes greater than about 20 degrees, and with heating restraints. The basic effect of propulsion during aerocruise is to (i) balance drag in order to maintain constant velocity, (ii) augment lift with a component of thrust, thus increasing cruising altitude over what it would be during aeroglide turn, and finally (iii) provide a lateral component of thrust giving the required turn necessary for plane change.

In this report, research has been conducted into cruise maneuver being performed using either bank control with constant thrust, or thrust control with constant bank control [26, 28].

II. SUMMARY/ABSTRACT OF RESEARCH WORK

(NASA Langley Grant NAG1-736)

SINGULAR PERTURBATION AND TIME SCALE APPROACHES IN DISCRETE CONTROL SYSTEMS*

Dr. D. S. Naidu
Dept. of Elect. and Computer Engineering
Old Dominion University
Norfolk, VA, 23508

and

Dr. D. B. Price
Spacecraft Control Branch
NASA Langley Research Center
Hampton, VA, 23665

Abstract: The theory of singular perturbations and time scales (SPaTS) has been a powerful analytical tool in the analysis and synthesis of continuous and discrete control systems. In this paper, we first consider a singularly perturbed discrete control system. Using singular perturbation approach, outer and correction subsystems are obtained. Next, by the application of time scale approach via block diagonalization transformations, the original system is decoupled into slow and fast subsystems. To a zeroth order approximation, the singular perturbation and time scale approaches yield equivalent results. Roughly speaking, the zeroth order approximation is sometimes called the first approximation. This result is similar to a corresponding result in continuous control systems.

* *See items 1 and 14 under List of Publications*

SINGULAR PERTURBATIONS AND TIME SCALES IN DISCRETE CONTROL SYSTEMS-AN OVERVIEW*

Dr. D. S. Naidu
Dept. of Elect. and Computer Engineering
Old Dominion University
Norfolk, VA, 23508

Dr. D. B. Price
Spacecraft Control Branch
NASA Langley Research Center
Hampton, VA, 23665

and

Dr. J. L. Hibey
Dept. of Elect. and Computer Engineering
Old Dominion University
Norfolk, VA, 23508

Abstract: This paper presents an overview of recent developments in the theory of singular perturbations and time scales (SPaTS) in discrete control systems. The focus is in three directions: modeling, analysis, and control. First, sources of discrete models and the effect of the discretizing interval on the modeling are reviewed. Then the analysis of two-time scale systems is presented to bring out typical characteristic features of SPaTS. Finally, in the control of the two-time scale systems, we the important issue of multirate sampling is addressed. The bibliography containing over 100 titles is included.

* *See items 2 and 8 under List of Publications*

ON THE METHOD OF MATCHED ASYMPTOTIC EXPANSIONS*

Dr. D. S. Naidu
Dept. of Elect. and Computer Engineering
Old Dominion University
Norfolk, VA, 23508

and

Dr. D. B. Price
Spacecraft Control Branch
NASA Langley Research Center
Hampton, VA, 23665-5225

Abstract: A critical examination of the method of matched asymptotic expansions (MAE) reveals that the various terms of the common solution of MAE can be generated as polynomials in stretched variable without actually solving for them from the outer solution as is done presently. This also shows that the common solution of the method of MAE and the intermediate solution of singular perturbation method are the same and hence that these methods give identical results for a certain class of problems. An illustrative example is given.

* *See items 3, 7 and 18 under List of Publications*

IMPACT OF ATMOSPHERIC DENSITY SCALE HEIGHT ON THE PERFORMANCE OF AEROASSISTED COPLANAR ORBITAL TRANSFER VEHICLES*

Dr. D. S. Naidu
Dept. of Elect. and Computer Engineering
Old Dominion University
Norfolk, VA, 23508

and

Dr. D. B. Price
Spacecraft Controls Branch
NASA Langley Research Center
Hampton, Virginia, 23665

Abstract: A common way of representing atmospheric density is by an exponential form using scale height, which is assumed to be constant over the whole interval of atmospheric altitude. In this simulation, the scale height has been readjusted depending upon the altitude interval, and simulations are carried out for an aeroassisted, coplanar orbital transfer vehicle.

* *See item 4 under List of Publications*

TIME-SCALE SYNTHESIS OF A CLOSED-LOOP DISCRETE OPTIMAL CONTROL SYSTEM*

Dr. D. S. Naidu
Dept. of Elect. and Computer Engineering
Old Dominion University
Norfolk, VA 23529

and

Dr. D. B. Price
Spacecraft Controls Branch
NASA Langley Research Center
Hampton, VA 23665-5225

Abstract: A two-time-scale discrete control system is considered. The closed-loop optimal linear quadratic regulator for the system requires the solution of a full-order algebraic matrix Riccati equation. Alternatively, the original system is decomposed into reduced-order slow and fast subsystems. The closed-loop optimal control of the subsystems requires the solution of two algebraic Riccati equations of an order lower than that required for the full-order system. A composite, closed-loop suboptimal control is created from the sum of the slow and fast feedback optimal controls. Numerical results obtained for an aircraft model show a very close agreement between the exact(optimal) solutions and computationally simpler composite(suboptimal) solutions. The main advantage of the method is the considerable reduction in the overall computational requirements for the closed-loop optimal control of digital flight systems.

* *See item 6 under List of Publications*

THREE-DIMENSIONAL ATMOSPHERIC ENTRY PROBLEM USING METHOD OF MATCHED ASYMPTOTIC EXPANSIONS*

Dr. D. S. Naidu
Dept. of Elect. and Computer Engineering
Old Dominion University
Norfolk, VA, 23508

Abstract: The analysis of a three-dimensional atmospheric entry problem using the method of matched asymptotic expansions is considered. A composite solution is formed in terms of an outer solution, an inner solution and a common solution. The outer solution is obtained from gravitationally dominant region, whereas the aerodynamically dominant region contributes to the inner solution. The common solution accounts for the overlap between the outer and inner regions. In comparison to the previous works, the present simplified methodology yields explicit analytical expressions for various components of the composite solution without resorting to any type of transcendental equations to be solved only by numerical methods. The method is applicable for obtaining autonomous guidance and control strategies for a variety of aerospace vehicles.

* *See items 9, 11 and 22 under List of Publications*

FUEL-OPTIMAL TRAJECTORIES FOR AEROASSISTED COPLANAR ORBITAL TRANSFER PROBLEM*

Dr. D. S. Naidu, Dr. J. L. Hibey, and C. Charalambous
Dept. of Electrical and Computer Engineering
Old Dominion University
Norfolk, VA, 23529

Abstract: We first describe briefly the various types of coplanar transfers. Then we address the fuel-optimal control problem arising in coplanar orbital transfer employing aeroassist technology. The maneuver involves a transfer from high Earth orbit to low Earth orbit and at the same time minimization of the fuel consumption for achieving the desired orbit transfer. It is known that a change in velocity, also called the characteristic velocity, is a convenient parameter to measure the fuel consumption. A suitable performance index is the total characteristic velocity which is the sum of the characteristic velocities for deorbit and for reorbit (or circularization). Use of Pontryagin minimum principle leads to a nonlinear, two-point boundary value problem in state and costate variables. The solution of the TPBVP is the stumbling block in obtaining fuel-optimal solution. This problem is solved by using a more efficient multiple shooting method which is a simultaneous application of a single shooting algorithm to equally divided points of the total interval of the solution.

* *See items 12, 17 and 25 under List of Publications*

FUEL-OPTIMAL TRAJECTORIES OF AEROASSISTED ORBITAL TRANSFER WITH PLANE CHANGE*

Dr. D. S. Naidu
Dept. of Elect. and Computer Engineering
Old Dominion University
Norfolk, VA, 23529

Abstract: The fuel-optimal control problem arising in noncoplanar orbital transfer employing aeroassist technology is addressed. The mission involves the transfer from high Earth orbit to low Earth orbit with plane change. The complete maneuver consists of a deorbit impulse to inject a vehicle from a circular orbit to elliptic orbit for the atmospheric entry, a boost impulse at the exit from the atmosphere for the vehicle to attain a desired orbital altitude and finally a reorbit impulse to circularize the path of the vehicle. In order to minimize the total fuel consumption, a performance index is chosen as the sum of the deorbit, boost, and reorbit impulses. Application of optimization principles leads us to a nonlinear, two-point, boundary value problem, which is solved by using a multiple shooting method.

* *See items 13, 19, 20 and 29 under List of Publications*

FUEL-OPTIMAL TRAJECTORIES FOR NONCOPLANAR ORBITAL TRANSFER VEHICLES*

Dr. D. S. Naidu
Dept. of Elect. and Computer Engineering
Old Dominion University
Norfolk, VA 23529

ABSTRACT: The fuel-optimal problem in noncoplanar orbital transfer employing aeroassist technology is addressed. The mission involves the transfer from high Earth orbit to low Earth orbit with plane change. The complete maneuver consists of a deorbit impulse to inject a vehicle from a circular orbit to elliptic orbit to enter the atmosphere, a boost impulse at the exit from the atmosphere for the vehicle to attain a desired orbital altitude and finally a reorbit impulse to circularize the path of the vehicle. In order to minimize the total fuel consumption, a performance index is chosen as the sum of the deorbit, boost, and reorbit impulses. For a typical aeroassisted orbital transfer vehicle with high lift-to-drag ratio, the simulations are carried out using industry standard program to optimize simulated trajectories (POST).

* *See item 15 under List of Publications*

SINGULAR PERTURBATIONS AND TIME SCALES IN THE DESIGN OF DIGITAL FLIGHT CONTROL SYSTEMS*

Dr. D. S. Naidu
Dept. of Elect. and Computer Engineering
Old Dominion University
Norfolk, VA 23529

and

Dr. Douglas B. Price
Spacecraft Controls Branch
NASA Langley Research Center
Hampton, VA 23665-5225

Abstract: This paper investigates the application of methodology of singular perturbations and time scales (SPaTS) to the control of digital flight systems. A block diagonalization method is developed to decouple a full-order, two-time (slow and fast) scale, discrete control system into reduced-order slow and fast subsystems. Basic properties and numerical aspects of the method are explored. This reveals an interesting fact that singularly perturbed discrete systems can be viewed as two-time scale systems. Next, the closed-loop optimal control of the two-time scale full-order system involves the solution of a full order algebraic matrix Riccati equation. Alternatively, using the block diagonalization method, the full-order system is decomposed into reduced-order slow and fast subsystems. The closed-loop optimal control of the subsystems requires the solution of only reduced-order algebraic matrix Riccati equations. A composite closed-loop suboptimal control is constructed as the sum of the slow and fast optimal feedback controls. Numerical experimentation with an aircraft model shows close agreement between the exact solutions and the decoupled (or composite) solutions. The main advantage of the method is the considerable reduction in the overall onboard computational requirements for the evaluation of optimal guidance and control laws. It is believed that this paper also serves as a source of brief survey of digital flight systems.

* *See item 16 under List of Publications*

NEIGHBORING OPTIMAL GUIDANCE FOR AN AEROASSISTED ORBITAL TRANSFER VEHICLE IN THE PRESENCE OF MODELLING UNCERTAINTIES*

Dr. D. S. Naidu, Dr. J. L. Hibey, and C. Charalambous
Dept. of Electrical and Computer Engineering
Old Dominion University
Norfolk, VA, 23529

ABSTRACT: We intend to devise a neighboring optimal guidance scheme for a nonlinear dynamic system with stochastic inputs and perfect measurements as applicable to fuel optimal control of an aeroassisted orbital transfer vehicle. For the deterministic nonlinear dynamic system describing the atmospheric maneuver, a nominal trajectory is determined. Then, a neighboring, optimal guidance scheme is obtained. Taking modelling uncertainties into account, a linear, stochastic, neighboring optimal guidance scheme is devised. Finally, the optimal trajectory is approximated as the sum of the deterministic nominal trajectory and the stochastic neighboring optimal solution. Numerical results are presented for a typical vehicle.

* *See items 23 and 27 under List of Publications*

NEIGHBORING OPTIMAL GUIDANCE FOR AEROASSISTED NONCOPLANAR ORBITAL TRANSFER*

D. S. Naidu
Dept. of Elect. and Computer Engineering
Old Dominion University
Norfolk, VA, 23508

Abstract: The fuel-optimal control problem in aeroassisted noncoplanar orbital transfer is addressed. The equations of motion for the atmospheric maneuver are nonlinear and the optimal (nominal) trajectory and control are obtained. In order to follow the nominal trajectory under actual conditions, a neighboring optimum guidance scheme is designed using linear quadratic regulator (LQR) theory for onboard real-time implementation. One of the state variables is used as the independent variable in preference to the time. The weighting matrices in the performance index are chosen by a combination of a heuristic method and an optimal modal approach. The necessary feedback control law is obtained in order to minimize the deviations from the nominal conditions.

* *See item 24 under List of Publications*

ORBITAL PLANE CHANGE MANEUVER WITH AEROCRUISE*

Dr. D. S. Naidu
Dept. of Electrical and Computer Engineering
Old Dominion University
Norfolk, VA

Abstract: The synergistic plane change problem connected with orbital transfer employing aeroassist technology, is addressed. The mission involves transfer from high Earth orbit to low Earth orbit with plane change being performed within the atmosphere. The complete mission consists of a deorbit phase, atmospheric phase, and finally reorbit phase. The atmospheric maneuver is composed of an entry mode, a cruise mode, and finally an exit mode. During the cruise mode, constant altitude and velocity are maintained by means of bank angle control with constant thrust or thrust control with constant bank angle. Comparisons between these two control strategies bring out some interesting features.

* *See items 26 and 28 under List of Publications*

III. LIST OF PUBLICATIONS

(NASA Langley Grant NAG1-736)

1. D. S. Naidu and D. B. Price, "Singular perturbation and time scale approaches in discrete control systems", in Research Report, Dept. of Elect. and Computer Engineering, Old Dominion University, Norfolk, VA, June 1987.

2. D. S. Naidu, et. al., "Singular perturbations and time scales in discrete control systems-an overview", in Research Report, Dept. of Elect. and Computer Engineering, Old Dominion University, Norfolk, VA, June 1987.

3. D. S. Naidu, and D. B. Price, "On the method of matched asymptotic expansions", in Research Report, Dept. of Elect. and Computer Engineering, Old Dominion University, Norfolk, VA, June 1987.

4. D. S. Naidu and D. B. Price, "Impact of atmospheric scale height on the performance of aeroassisted orbiter transfer vehicles", in Research Report, Dept. of Elect. and Computer Engineering, Old Dominion University, Norfolk, VA, June 1987.

5. L. W. Taylor, Jr., and D. S. Naidu, "Experience in distributed parameter modeling of the spacecraft control laboratory experiment (SCOLE) structure", AIAA Dynamics Specialists Conference, Monterey, CA, April 1987.

6. D. S. Naidu and D. B. Price, "Time scale synthesis of a closed-loop discrete optimal control system", Journal of Guidance, Control, and Dynamics, 10, 417-421, Sept.-Oct. 1987.

7. D. S. Naidu, and D. B. Price, "On the method of matched asymptotic expansions", SIAM Annual Meeting and 35th Anniversary, Denver, CO, October 12-15, 1987

8. D. S. Naidu, et. al., "Singular perturbations and time scales in discrete control systems-an overview", Survey Paper at the Invited Session, IEEE Conference on Decision and Control, Los Angles, CA, Dec. 9-11, 1987

9. D. S. Naidu, "There-dimensional atmospheric entry problem using method of matched asymptotic expansions", in Research Report, Dept. of Elect. and Computer Engineering, Old Dominion University, Norfolk, VA, December 1987.

10. D. S. Naidu, Singular Perturbation Methodology in Control Systems, IEE Control Engineering Series, Peter Peregrinus Ltd., Stevenage Herts, England, 1988.

11. D. S. Naidu, "There-dimensional atmospheric entry problem using method of matched asymptotic expansions", 1988 American Control Conference, Atlanta, GA, June 14-17, 1988.

12. D. S. Naidu, et. al., "Fuel-optimal trajectories for aeroassisted, coplanar, orbital transfer problem", Research Report, Dept. of Elect. and Computer Engineering, Old Dominion University, Norfolk, VA, June, 1988.

13. D. S. Naidu, "Fuel-optimal trajectories for aeroassisted, noncoplanar, orbital transfer problem", Research Report, Dept. of Elect. and Computer Engineering, Old Dominion University, Norfolk, VA, June, 1988.

14. D. S. Naidu and D. B. Price, "Singular perturbation and time scale approaches in discrete control systems", Journal of Guidance, Control and Dynamics, Vol., 11, no. 5, pp. 592-594, Nov.-Dec. 1988.

15. D. S. Naidu, "Fuel-optimal trajectories for noncoplanar orbital transfer vehicles", Research Report, Dept. of Elect. and Computer Engineering, Old Dominion University, Norfolk, VA, December 1988.

16. D. S. Naidu and D. B. Price, "Singular Perturbations and Time Scales in the Design of Digital Flight Control Systems", NASA Technical Paper 2844, Langley Research Center, Hampton, December 1988

17. D. S. Naidu, et. al., "Optimal control of aeroassisted, coplanar, orbital transfer vehicles", 26th IEEE Conference on Decision and Control, Austin, Texas, December 7-9, 1988.

18. D. S. Naidu and D. B. Price, "On the method of matched asymptotic expansions", Journal of Guidance, Control, and Dynamics, 12, 277-279, March-April 1989.

19. D. S. Naidu, "Fuel-optimal trajectories of aeroassisted orbital transfer with plane change," in Research Report, Dept. of Elect. and Computer Engineering, Old Dominion University, Norfolk, VA, June 1989.

20. D. S. Naidu, "Fuel-optimal trajectories of aeroassisted orbital transfer with plane change," AIAA Guidance, Navigation, and Control Conference, Boston, MA, August 14-16, 1989.

21. D. S. Naidu, and Anthony J. Calise, "Singular perturbations and time scales in control theory and applications: survey 1983-1989", IFAC Workshop on Singular Perturbations and Asymptotic Methods in Systems and Control, Boston, MA, Aug. 17-18, 1989.

22. D. S. Naidu, "There-dimensional atmospheric entry problem using method of matched asymptotic expansions", IEEE Trans. on Aerospace and Electronic Systems, 25, 660-667, Sept. 1989.

23. D. S. Naidu, et. al., "Fuel-optimal trajectories for aeroassisted coplanar orbital transfer vehicles in the presence of uncertainties due to modelling inaccuracies", in Research Report, Dept. of Electrical and Computer Engineering, Old Dominion University, Norfolk, VA, December 1989

24. D. S. Naidu, "Neighboring optimal guidance for aeroassisted noncoplanar orbital transfer", in Research Report, Dept. of Electrical and Computer Engineering, Old Dominion University, Norfolk, VA, December 1989

25. D. S. Naidu, et. al., "Fuel-optimal trajectories for aeroassisted coplanar orbital transfer problem", IEEE Trans. on Aerospace and Electronic Systems, 26, 374-381, March 1990.

26. D. S. Naidu, "Orbital plane change maneuver with aerocruise", in Research Report, Dept. of Elect. and Computer Engineering, Old Dominion University, Norfolk, VA July, 1990

27. D. S. Naidu, et. al., "Neighboring optimal guidance for an aeroassisted orbital transfer vehicle in the presence of modelling uncertainties", AIAA Guidance, Control, and Navigation Conference, Portland, OR, August 20-22, 1990

28. D. S. Naidu, "Orbital plane change maneuver with aerocruise", accepted for presentation at AIAA 29th Aerospace Science Meeting and Exhibit, Reno, Nevada, January 7-10, 1991.

29. D. S. Naidu, "Fuel-optimal trajectories of aeroassisted orbital transfer with plane change," IEEE Trans. Aerospace and Electronic Systems, 27, May 1991 (in press).

GUIDANCE AND CONTROL STRATEGIES FOR AEROSPACE VEHICLES

(NASA Langley Grant NAG1-736)

PART II

This final report under NASA Langley grant NAG1-736 consists of two parts. Part I consists of the summary of the earlier work whose reports have been submitted at various times during the period (1/1/87 to 12/31/1989). Part II describes in detail the research work done during the period 1/1/1990 to 7/31/1990.

ORBITAL PLANE CHANGE MANEUVER WITH AEROCRUISE

Dr. D. S. Naidu
Dept. of Electrical and Computer Engineering
Old Dominion University
Norfolk, VA

Address for correspondence: Dr. D. S. Naidu
Spacecraft Control Branch, MS 161
NASA Langley Research Center
Hampton, VA, 23665-5225
Ph: (804) 864-6498

TABLE OF CONTENTS

		Page
	ABSTRACT	2
	NOMENCLATURE	2
I.	INTRODUCTION	4
II.	MISSION DESCRIPTION	7
III.	DESCENT MODE	9
IV.	AEROCRUISE MODE: BANK ANGLE CONTROL	14
V.	AEROCRUISE MODE: THRUST CONTROL	22
VI.	ASCENT MODE	26
VII.	BOOST AND REORBIT PHASE	29
VIII.	NUMERICAL DATA AND RESULTS	30
IX.	CONCLUDING REMARKS	34
X.	REFERENCES	35

LIST OF FIGURES

Page

1. Aeroassisted Orbital Transfer Mission.....37

2. Atmospheric Phase.....38

3. Coordinate System.....39

4. Lift and Drag Coefficients.....40

5. Lift-to-Drag Ratio and Aeropropulsive Efficiency.....41

6(a). Altitude as a Function of Time during Descent Mode.....42

6(b). Velocity as a Function of Time during Descent Mode.....43

6(c). Flight Path Angle as a Function of Time During Descent Mode.....44

7. Optimum Thrust Angle as a Function of Angle of Attack.....45

8. Maximum Heading Angle as a Function of Angle of Attack.....46

9(a). Mass as a Function of Time with Bank Angle Control.....47

9(b). Bank Angle as a Function of Time with Bank Angle Control.....48

9(c). Heading Angle as a Function of Time with Bank Angle Control.....49

10. Optimum Bank Angle as a Function of Angle of Attack.....50

11. Maximum Heading Angle as a Function of Angle of Attack.....51

12(a). Mass as a Function of Time with Thrust Control.....52

12(b). Thrust as a Function of Time with Thrust Control.....53

12(c). Thrust Angle as a Function of Time with Thrust Control.....54

12(d). Heading Angle as a Function of Time with Thrust Control.....55

13. Maximum Heading Angle as a Function of Angle of Attack.....56

14(a). Altitude as a Function of Time During Ascent Mode.....57

14(b). Velocity as a Function of Time During Ascent Mode.....58

14(c). Flight Path Angle as a Function of Time During Ascent Mode.....59

15(a). Altitude as a Function of Time with Bank Angle Control.....60

15(b). Velocity as a Function of Time with Bank Angle Control.....61

15(c). Flight Path Angle as a Function of Time with Bank Angle Control..62

15(d). Heading Angle as a Function of Time with Bank Angle Control.....63

15(e). Heat Rate as a Function of Time with Bank Angle Control.....64

16(a). Altitude as a Function of Time with Thrust Control.....65

16(b). Velocity as a Function of Time with Thrust Control.....66

16(c). Flight Path Angle as a Function of Time with Thrust Control.....67

16(d). Heading Angle as a Function of Time with Thrust Control.....68

16(e). Heat Rate as a Function of Time with Thrust Control.....69

ORBITAL PLANE CHANGE MANEUVER WITH AEROCRUISE

Dr. D. S. Naidu
Dept. of Electrical and Computer Engineering
Old Dominion University
Norfolk, VA

Address for correspondence: Dr. D. S. Naidu
Spacecraft Control Branch, MS 161
NASA Langley Research Center
Hampton, VA, 23665-5225
Ph: (804) 864-6498

Abstract: The synergistic plane change problem connected with orbital transfer employing aeroassist technology, is addressed. The mission involves transfer from high Earth orbit to low Earth orbit with plane change being performed within the atmosphere. The complete mission consists of a deorbit phase, atmospheric phase, and finally reorbit phase. The atmospheric maneuver is composed of an entry mode, a cruise mode, and finally an exit mode. During the cruise mode, constant altitude and velocity are maintained by means of bank angle control with constant thrust or thrust control with constant bank angle. Comparisons between these two control strategies bring out some interesting features.

Nomenclature

C_D : drag coefficient
C_{DO} : drag coefficient at zero lift
C_L : lift coefficient
C_{LR} : lift coefficient for maximum lift-to-drag ratio
D : drag force
E : maximum value of lift-to-drag ratio
E_p : aeropropulsive efficiency
g : gravitational acceleration
H : altitude
$\mathcal{H}$: Hamiltonian
I_{sp} : specific fuel consumption
i : inclination
J : performance index
K : induced drag factor
L : lift force
m : vehicle mass
Q : Heating rate
R : distance from Earth center to vehicle center of gravity
R_E : radius of Earth
S : aerodynamic reference area
T : thrust
t : time

V : velocity

α : angle of attack

β : inverse atmospheric scale height

γ : flight path angle

δ : normalized density

ζ = normalized lift coefficient

η : thrust angle

θ : down range angle

λ : costate (Langrange) variable

μ : gravitational constant of Earth

ρ : density

σ : bank angle

ϕ : cross range angle

ψ : heading angle

ΔV : characteristic velocity

Subscripts

a : atmospheric boundary

c : circularization at LEO

d : deorbit at HEO

e : entry to atmosphere

f : exit from atmosphere

j : beginning of aerocruise

n : end of aerocruise

s : surface level

I. INTRODUCTION

The main function of space transportation system is to deliver payloads from Earth to various locations in space. Until now, this function has been performed by various rockets, the space shuttle, and expendable upper stages using solid or liquid propellants. In particular, considering the economic benefits and reusability, an orbital transfer vehicle (OTV) is proposed for transporting payloads between low Earth orbit (LEO) and high Earth orbit (HEO).[1] The two basic operating modes contemplated for OTV are a ground-based OTV which returns to Earth after each mission and a space-based OTV which operates out of an orbiting hanger located at the proposed Space Station Freedom.

In a typical mission, a space-based OTV, which is initially at the space station orbit (SSO), is required to transfer a payload to geosynchronous Earth orbit (GEO), pick up another payload, say a faulty satellite, and return to rendezvous with the orbiting hanger at SSO for refurbishment and redeployment of payload. The OTV on its return journey from GEO to SSO needs to dissipate some of its orbital energy. This can be accomplished by using an entirely propulsive (Hohmann) transfer in space only or a combination of propulsive transfer in space and aeroassisted maneuver in the atmosphere. It has been established that a significant fuel savings and hence increased payload capabilities can be achieved with propulsive and aeroassisted maneuvers instead of all-propulsive maneuvers.[1] This leads to an aeroassisted orbital transfer vehicle (AOTV), which on its return leg of the mission, dips into the Earth's atmosphere, utilizes atmospheric drag to reduce orbital velocity and to achieve a desired orbital inclination. Basically, the AOTV performs a synergistic maneuver, employing a hybrid combination of propulsive maneuver in space and aerodynamic maneuver in the atmosphere.

The plane change capability is required to (i) orbit a vehicle in a plane which does not pass through a launch site, (ii) shorten the time needed to reach multiple reconnaissance targets on a single orbital mission, (iii) reduce the time needed to return to base from orbit, (iv) perform effective rendezvous with satellites in different orbital planes, (v) avoid flights over hostile territory, and finally (vi) facilitate arrival and departure flights

from Space Station Freedom, in fulfilling specified mission objectives.[2] It should be noted that an orbital plane is usually defined in terms of inclination and longitude of the ascending node. For our present purpose only an inclination change is controlled.

There are basically three methods of plane change, (i) impulsive method, (ii) aeroglide method, and (iii) aerocruise method. In impulsive method, the plane change is achieved entirely outside the atmosphere, and fuel consumption is prohibitively large for sizable changes of orbital plane. In both aeroglide and aerocruise methods, rockets are used to deflect the vehicle into the atmosphere, and the plane change is accomplished by heading change of the vehicle. With aeroglide there is no thrusting during the atmosphere, and with aerocruise, atmospheric drag is balanced by a continuous thrust to keep the spacecraft at a constant altitude and velocity. Propellent expenditure comparisons among the three methods of plane change show that the aerocruise method is superior to other competing methods for plane changes greater than about 20 degrees, and with heating restraints. The basic effect of propulsion during aerocruise is to (i) balance drag in order to maintain constant velocity, (ii) augment lift with a component of thrust, thus increasing cruising altitude over what it would be during aeroglide turn, and finally (iii) provide a lateral component of thrust giving the required turn necessary for plane change. The aeroglide and aerocruise methods utilizing atmospheric maneuver in conjunction with propulsion augmentation are also termed the "synergistic" or "aeropropulsive" methods.[3,4]

The following are some of the features of atmospheric plane change.[5-7] (i) For plane changes of less than 15 degrees, an all-propulsive maneuver is generally more efficient. (ii) An L/D of at least 2 is required to offer a significant advantage over the all-propulsive plane change, and it is desirable to maximize the L/D of a vehicle. (iii) A plane change made at a node produces all inclination change whereas a turn at an orbit apex (90 degrees from node) provides no inclination change, only a shift in the node. Hence, for maximum inclination change and minimum node shift, the turn should be centered over the node in the shortest possible duration. Thus, plane changes performed at maximum C_L (i.e., high angle of attack) which are quicker are more fuel efficient than the slower maximum L/D turns. (iv) The total heat

load can be reduced substantially by carrying out a quicker high angle-of-attack turns rather than the slower maximum L/D turns. (v) An aerocruise (thrusting) turn offers significant advantages over an aeroglide (non-thrusting) turn, when the desired plane change is more than 10 degrees. (vi) During aerocruise, the high angle-of-attack and bank attitude of the vehicle produce a lateral component of thrust, which is responsible for a significant amount of plane change.

Compared to other works,[5-8] the highlights of the present work are (i) The analysis covers the complete mission from HEO to LEO. (ii) The descent mode and ascent mode of atmospheric phase are analyzed with flight path angle as an independent variable. (iii) The time has been retained as an independent variable during the cruise mode. (iv) During the cruise mode, both bank angle control and thrust control are analyzed.

In this report, we address the synergistic plane change problem arising in noncoplanar orbital transfer employing aeroassist technology. The mission involves the transfer from HEO to LEO with plane change being performed within the atmosphere. The complete mission consists of a deorbit phase, an atmospheric phase, and finally a reorbit phase. The atmospheric maneuver phase is composed of descent (entry) mode, cruise mode, and ascent (exit) mode. During the aerocruise mode, constant altitude and velocity are maintained either by (i) varying bank angle with constant thrust, or by (ii) varying thrust with constant bank angle. The comparison of these two control schemes bring out some interesting features. Numerical results are given for typical data.

II. MISSION DESCRIPTION

For an orbital transfer problem, the following assumptions are made. (i) The initial HEO and final LEO orbits are circular. (ii) The mission is comprised of three impulses. (iii) The vehicle is represented as a constant point mass during atmospheric pass. (iv) A Newtonian inverse square gravitational field is used. (v) Earth's rotation is neglected. (vi) The atmosphere is exponential.

The complete mission from HEO to LEO with atmospheric pass is depicted in Fig. 1. It consists of a deorbit phase, an atmospheric phase, and a reorbit phase. There are three impulses: first, a deorbit impulse ΔV_d at HEO to inject a vehicle into a HEO-entry elliptic orbit, second, a boost impulse ΔV_b at the exit from the atmosphere for the vehicle to attain sufficient velocity to travel along an exit-LEO elliptic orbit, and finally, a circularizing impulse ΔV_c to circularize the path of the vehicle. The atmospheric phase itself is composed of descent (entry) mode, cruise mode, and ascent (exit) mode.

Consider the basic equations of motion for different phases of deorbit, aeroassist (or atmospheric flight), boost and reorbit (or circularization).

Deorbit Phase

Initially, we assume that a spacecraft is in a circular orbit of radius R_d, well outside the Earth's atmosphere, moving with a circular velocity $V_d = \sqrt{\mu/R_d}$. Deorbit is performed by means of an impulse ΔV_d, to transfer the vehicle from the circular orbit to elliptic orbit with perigee low enough to intersect the dense part of the atmosphere [Fig. 1]. At D, since the elliptic velocity is less than the circular velocity, the impulse ΔV_d is executed so as to oppose the circular velocity V_d. The deorbit impulse ΔV_d causes the vehicle to enter the atmosphere of radius R_a with a velocity V_e and flight path angle γ_e. It is known that the optimal-energy loss maneuver from the circular orbit is simply the Hohmann transfer and the impulse is parallel and opposite to the instantaneous velocity vector.

Using the principle of conservation of energy and angular momentum at the

deorbit point D, and the atmospheric entry point E, we get,[9]

$$V_e^2/2 - \mu/R_a = (V_d - \Delta V_d)^2/2 - \mu/R_d \tag{1}$$

$$R_a V_e \cos(-\gamma_e) = R_d(V_d - \Delta V_d) \tag{2}$$

from which solving for ΔV_d, we get

$$\Delta V_d = \sqrt{\mu/R_d} - \sqrt{2\mu(1/R_a - 1/R_d)/\left[(R_d/R_a)^2/\cos^2\gamma_e - 1\right]} \tag{3}$$

It is easily seen that the minimum value of the deorbit impulse ΔV_{dm} obtained at $\gamma_e = 0$, corresponds to an ideal transfer wherein the space vehicle grazes along the atmospheric boundary. To ensure proper atmospheric entry, the deorbit impulse ΔV_d must be higher than the minimum deorbit impulse ΔV_{dm} which is given by

$$\Delta V_{dm} = \sqrt{\mu/R_d} - \sqrt{2\mu(1/R_a - 1/R_d)/\left[(R_d/R_a)^2 - 1\right]} \tag{4}$$

Aeroassist (Atmospheric) Phase

The atmospheric phase of the mission is composed of (i) descent mode, (ii) cruise mode, and (iii) ascent mode [Fig. 2].

III DESCENT MODE

During the descent mode, the equations of motion for the vehicle (without any thrusting) are given below [Fig. 3]. The kinematic equations are,[10]

$$\frac{dR}{dt} = V\sin\gamma \tag{5a}$$

$$\frac{d\theta}{dt} = V\cos\gamma\cos\psi/R\cos\phi \tag{5b}$$

$$\frac{d\phi}{dt} = V\cos\gamma\sin\psi/R \tag{5c}$$

The force equations are

$$m\frac{dV}{dt} = -D - mg\sin\gamma \tag{5d}$$

$$mV\frac{d\gamma}{dt} = L\cos\sigma + m(V^2/R - g)\cos\gamma \tag{5e}$$

$$mV\frac{d\psi}{dt} = L\sin\sigma/\cos\gamma - (mV^2/R)\cos\gamma\cos\psi\tan\phi \tag{5f}$$

where,

$$L = C_L(\alpha)\rho SV^2/2; \quad D = C_D(\alpha)\rho SV^2/2; \quad C_D = C_{DO} + KC_L^2$$

$$g = \mu/R^2; \quad R = H + R_E; \quad \rho = \rho_s\exp(-\beta H)$$

Neglecting mass terms in comparison to aerodynamic terms in (5), we get

$$\frac{dH}{dt} = V\sin\gamma \tag{6a}$$

$$\frac{dV}{dt} = -D/m \tag{6b}$$

$$\frac{d\gamma}{dt} = L\cos\sigma/mV \tag{6c}$$

$$\frac{d\psi}{dt} = L\sin\sigma/mV\cos\gamma \tag{6d}$$

Using flight path angle as the independent variable, we get

$$\frac{dH}{d\gamma} = 2m\exp(\beta H)\sin\gamma/\rho_0 SC_L\cos\sigma \tag{7a}$$

$$\frac{dV}{d\gamma} = - C_D V/C_L\cos\gamma \tag{7b}$$

$$\frac{d\psi}{d\gamma} = \tan\sigma/\cos\gamma \tag{7c}$$

During the descent mode, let us assume that there is no banking of the vehicle, and hence no heading is achieved. Then (7) becomes

$$\frac{dH}{d\gamma} = 2m\exp(\beta H)\sin\gamma/\rho_0 SC_L \tag{8a}$$

$$\frac{dV}{d\gamma} = - C_D V/C_L \tag{8b}$$

Optimal Control Problem

The optimal control problem is posed as follows. Given entry conditions, and the conditions at the end of the descent mode (or the initiation of aerocruise mode), find the optimal control law which maximizes the final velocity, subject to altitude constraint $H \geq H_b$.[11] This altitude constraint implies in a way heat-rate constraint. The performance index is given by

$$J = - V_b \tag{9}$$

The Hamiltonian for (8) and (9) is

$$\mathcal{H} = \lambda_H\left[2m\exp(\beta H)\sin\gamma/\rho_0 SC_L\right] + \lambda_v\left[- C_D V/C_L\right] \tag{10}$$

The adjoint equations are

$$d\lambda_H/d\gamma = -\lambda_H 2m\beta\exp(\beta H)\sin\gamma/\rho_0 SC_L \tag{11a}$$

$$d\lambda_v/d\gamma = \lambda_v C_D/C_L \tag{11b}$$

Solving the state (8) and costate (11) equations, we get

$$V\lambda_v = V_e\lambda_{ve} = \text{constant} \tag{12a}$$

$$\lambda_H\exp(\beta H) = \lambda_{He}\exp(\beta H_e) \tag{12b}$$

The boundary conditions for the adjoint variables are

$$\lambda_v(\gamma = \gamma_j) = \left.\frac{\partial J}{\partial V}\right|_{\gamma = \gamma_j} = -1 \tag{13a}$$

$$\lambda_H(\gamma = \gamma_j) = \left.\frac{\partial J}{\partial H}\right|_{\gamma = \gamma_j} = 0 \tag{13b}$$

From (12) and (13),

$$\lambda_H = 0 \tag{14}$$

With (14), the Hamiltonian (10) reduces to

$$\mathcal{H} = -\lambda_v V[C_{DO}/C_L + KC_L] \tag{15}$$

The optimal control is then given by

$$\frac{\partial \mathcal{H}}{\partial C_L} = 0 \tag{16}$$

leading to

$$C_{LO} = \sqrt{C_{DO}/K} = C_{LE} \tag{17}$$

where, C_{LE} is the lift coefficient for maximum lift-to-drag ratio $(L/D)_{max} = E$

$= 1/2\sqrt{KC_{DO}}$. With optimal control (17) in (8), we solve for the velocity and altitude as

$$V(\gamma) = V_e \exp[-(\gamma-\gamma_e)/E] \tag{18}$$

$$H = \ln\left[\exp(-\beta H_e) + \frac{2\beta m}{\rho_0 S C_{LO}}(\cos\gamma - \cos\gamma_e)\right]^{-1/\beta} \tag{19a}$$

For small γ, (19) reduces to

$$H = \ln\left[\exp(-\beta H_e) - \frac{\beta m}{\rho_0 S C_{LO}}(\gamma^2 - \gamma_e^2)\right]^{-1/\beta} \tag{19b}$$

At the start of the descent mode, $\gamma = \gamma_e$, and at the end of the descent mode (or the beginning of the aerocruise mode), $\gamma = \gamma_j = 0$. Then the above relations become

$$H_j = \ln\left[\exp(-\beta H_e) + \frac{2\beta m}{\rho_0 S C_{LO}}(1 - \cos\gamma_e)\right]^{-1/\beta} \tag{19c}$$

and with the approximation,

$$H_j = \ln\left[\exp(-\beta H_e) + \frac{\beta m}{\rho_0 S C_{LO}}\gamma_e^2\right]^{-1/\beta} \tag{19d}$$

Then, the inequality constraint on altitude $H \geq H_j$, with (19a) transforms to

$$\gamma_e \leq \cos^{-1}\left[1 - \frac{\rho_0 S C_{LO}}{2m\beta}\left\{\exp(-\beta H_j) - \exp(-\beta H_e)\right\}\right] \tag{20a}$$

and with approximate solution (19b),

$$\gamma_e^2 \leq \frac{\rho_0 S C_{LO}}{m\beta}\left[\exp(-\beta H_j) - \exp(-\beta H_e)\right] \tag{20b}$$

The velocity at the end of the descent mode is obtained from (18) with $\gamma = \gamma_j = 0$ as

$$V_j = V_e \exp\left(2\gamma_e \sqrt{C_{DO} K}\right) \tag{21}$$

IV. AEROCRUISE MODE: BANK ANGLE CONTROL

We first write down the general equations of motion, inject the conditions for cruise flight, use the assumptions of small latitude, and finally optimize the heading change. During aerocruise mode, there is continuous thrusting. Thus the kinematic equations are [Fig. 3][10]

$$\frac{dH}{dt} = V\sin\gamma \tag{22a}$$

$$\frac{d\theta}{dt} = V\cos\gamma\cos\psi/R\cos\phi \tag{22b}$$

$$\frac{d\phi}{dt} = V\cos\gamma\sin\psi/R \tag{22c}$$

The force equations are

$$m\frac{dV}{dt} = T\cos\eta - D - mg\sin\gamma \tag{22d}$$

$$mV\frac{d\gamma}{dt} = (T\sin\eta + L)\cos\sigma + m(V^2/R - g)\cos\gamma \tag{22e}$$

$$mV\frac{d\psi}{dt} = (T\sin\eta + L)\sin\sigma/\cos\gamma - (mV^2/R)\cos\gamma\cos\psi\tan\phi \tag{22f}$$

The propulsion (thrusting) equation is

$$\frac{dm}{dt} = -T/gI_{sp} \tag{22g}$$

From the above equations of motion, we see clearly that during the atmospheric maneuver, if the lift vector L is rotated about the velocity vector V through the bank angle σ, it creates a lateral force component $(T\sin\eta + L)\sin\sigma$ orthogonal to the vertical plane that has the effect of changing the heading angle ψ. At the end of the atmospheric phase, the equations (22c) and (22f) for the cross range angle ϕ, and the heading angle ψ, become,[10]

$$\frac{d\phi/dt}{d\psi/dt} = -\frac{\tan\psi}{\tan\phi} \tag{23a}$$

integration of which yields,

$$\cos\phi\cos\psi = \cos i \tag{23b}$$

where, i is the orbital inclination. For small values of cross range angle ϕ, the orbital inclination i is given by the heading angle ψ itself. Thus, the total change in the heading corresponds to the change in orbital inclination (plane change).

Now let us insert the cruise conditions of constant altitude and velocity.[8] The constant altitude condition on (22a) gives zero flight path angle throughout. The constant velocity condition on (22d) boils down to

$$T\cos\eta = D = \rho S V^2 C_D(\alpha)/2 \tag{24a}$$

We note that the conditions at the beginning of the aerocruise mode are denoted by the subscript j. However, for simplicity in notation we shall continue to use the variables without any subscript to denote the cruise conditions. If the angle of attack α is held constant, then the drag force D is constant at a constant cruising altitude. Also, since the flight path angle is zero throughout, (22e) reduces to

$$(T\sin\eta + L)\cos\sigma = m(g - V^2/R) \tag{24b}$$

Combining (24a) and (24b), we get

$$\cos\sigma = \frac{m(g - V^2/R)\cos\eta}{D[\sin\eta + (L/D)\cos\eta]} \tag{25}$$

where,

$$\sin\eta + (L/D)\cos\eta = (L + T\sin\eta)/T = E_p \tag{26}$$

is called aeropropulsive efficiency. Alternatively,

$$(D\tan\eta + L)\cos\sigma = m(g - V^2/R) \tag{27a}$$

The above equation is also rewritten as

$$\tan\eta = mK_1/\cos\sigma - L/D \tag{27b}$$

$$\text{where, } K_1 = (g - V^2/R)/D = (gR - V^2)/RD \tag{27c}$$

From (24a), we see that for a given angle of attack α, if altitude H, and velocity V are kept constant, then the drag D and lift L forces are constant. The mass m always changes due to thrusting. Then the above relation (27b) for variable mass can be satisfied in any one of the following three ways.

(i) Variable bank angle with constant angle of attack and thrust angle: With bank control, (22g) and (27a) mean that the thrust T is constant leading to a constant mass flow rate.

(ii) Variable thrust with constant bank angle: On the other hand, with thrust control, (24) implies that we need to change both magnitude and angle of the thrust, in order to keep a constant drag force. Thus for cruise condition, both thrust magnitude and angle need to be controlled such that $T\cos\eta$ is constant, but $T\sin\eta$ changes according to (24b) [see Fig. 3]. This leads to variable mass flow rate.

(iii) Variable bank angle and variable thrust: Here, we change both bank angle and thrust magnitude and angle, in order to satisfy the cruise conditions (24a) and (24b). This also leads to variable mass flow rate.

Obviously, the bank angle control leading to constant thrust (and hence constant mass flow rate) seems to be the simplest of all for implementation. However, it will be interesting to see which of the control schemes provides greatest amount of heading change and thereby inclination for the same amount of fuel expenditure.

The bank angle control with constant thrust magnitude and angle has been thoroughly discussed using arc length as independent variable.[8] However, in our present work, we continue to use time as independent variable. Assuming the latitude to be small, the cruise motion is described by

$$\frac{d\theta}{dt} = V\cos\psi/R \tag{28a}$$

$$\frac{dm}{dt} = -K_2/\cos\eta \tag{28b}$$

$$\frac{d\psi}{dt} = K_3\tan\sigma \tag{28c}$$

$$K_2 = D/gI_{sp}\ ; \qquad K_3 = g/V - V/R \tag{28d}$$

The bank angle control is given by

$$\cos\sigma = mK_1/[\tan\eta + L/D] = mK_4 \tag{29a}$$

where,

$$K_4 = \frac{(g - V^2/R)}{(L + D\tan\eta)} = \frac{2(k^2 - 1)}{\rho RSC_D(\alpha)[\tan\eta + L/D]} \tag{29b}$$

and $k = \sqrt{gR/V}$, the ratio of circular speed to cruise speed at R. From (29), we see that for a given angle of attack, and at constant altitude, speed, and thrust angle, the bank angle has to be varied as per the mass. That is, as mass m decreases along the flight, bank angle σ should be increased. Thus, in increasing the bank angle with the decrease of mass, we are trying to balance the decrease in the difference between the vehicle's weight and centrifugal force with the sum of vertical components of lift and thrust. In this control scheme, both mass and bank angle change, whereas altitude, velocity, angle of attack, thrust, thrust angle, and mass flow rate are held constant.

The cruise condition (29) reveals that

(a) With $\sigma = 0^0$, there is no banking and the cruise conditions can be maintained only by variable thrusting.

(b) For $0 < \sigma < 90^0$, the cruising speed is less than circular speed. The lift is directed upward. The gravitational force is higher than the centrifugal force.

(c) $\sigma = 90^0$ corresponds to cruise speed being equal to the circular speed, and all the aerodynamic force ($T\sin\eta + L$) is used for heading change or turning. The gravitational force is equal to the centrifugal force.

(d) For $\sigma > 90^0$, the cruising speed is higher than the circular speed. The centrifugal force is higher than the gravitational force and hence the lift is directed downward in order to prevent the vehicle to escape from Earth.

Given the initial values of mass m_j, and heading angle ψ_j, we find the initial bank angle σ_j from (29a). Also, we can solve (28b) directly as

$$m(t) = -(K_2/\cos\eta)t + m_j \tag{30}$$

Thus, $\sigma(t)$, and $\psi(t)$ are solved until either of the desired final conditions m_n, or ψ_n is realized. With a constant thrust angle η, and given initial mass m_j, and heading angle ψ_j, and final mass m_n (or final heading angle ψ_n) the sequence of solution of the aerocruise problem is to solve, first the mass equation (28b), second the bank angle equation (29a), and finally the heading angle equation (28c).

In this formulation for aerocruise, we see that the heading angle changes with respect to bank angle as given by (28c), and bank angle in turn has to follow the mass as per (29a), and the mass varies independently according to (30). Hence, there is no optimization of heading angle w.r.t. bank angle control variable, for a given fuel consumption or of fuel consumption w.r.t. bank angle control variable, for a given heading change. Alternatively, from (29) and (30), we can solve for ψ, which is now a function of thrust angle η, cruising altitude H, and cruising speed V. Then, we can find the optimal value

of η, which should be maintained constant throughout the aerocruise to achieve maximum ψ.

Optimization of Heading Change w.r.t. Thrust Angle

The optimization problem here is to find an optimum thrust angle which is to kept constant throughout the cruise mode, in order to maximize the heading change. We can solve this problem in a variety of ways. Basically, the heading angle ψ can be solved from (28) to (30) in terms of time t, mass m, or bank angle σ. Thus,

$$\psi_n = \psi_j + K_S\left[\ln(A_n/A_j) + B_j - B_n\right] \tag{31a}$$

where,

$$K_S = \frac{I_{sp}g}{V}\left[\sin\eta + (L/D)\cos\eta\right] \tag{31b}$$

$$A_i = (1 + \sin\sigma_i)/\cos\sigma_i; \quad B_i = \sin\sigma_i; \quad i = j,\ n \tag{31c}$$

Note that A_i, and B_i can also be expressed in terms of mass m using (29), or in terms of time t with (30). For example, in terms of mass m, (31c) becomes

$$A_i = \frac{\left[1 + \sqrt{1 - (m_i K_4)^2}\right]}{m_i K_4}; \quad B_i = \sqrt{1 - (m_i K_4)^2}; \quad i = j,\ n \tag{31d}$$

In terms of bank angle σ, (31) is rewritten as,[11]

$$\psi_n = \psi_j + \frac{I_{sp}g}{V}\left[\sin\eta + (L/D)\cos\eta\right]\left[\ln\left\{\frac{\cos\sigma_j(1 + \sin\sigma_n)}{\cos\sigma_n(1 + \sin\sigma_j)}\right\} + \sin\sigma_j - \sin\sigma_n\right] \tag{32}$$

where, bank angle σ is related with thrust angle η as per (29). Now optimizing ψ_n with respect to thrust angle η, (i.e., making $d\psi_n/d\eta = 0$) and assuming the initial value $\psi_j = 0$, we get

$$\cos\eta[\cos\eta + (L/D)\sin\eta]\left[\ln\left\{\frac{\cos\sigma_j(1 + \sin\sigma_n)}{\cos\sigma_n(1 + \sin\sigma_j)}\right\} + \sin\sigma_j - \sin\sigma_n\right] = 0 \qquad (33)$$

Using first order approximations in the change of the bank angle,

$$\cos\sigma_n = \cos(\sigma_j + \Delta\sigma) \cong \cos\sigma_j - (\sin\sigma_j)\Delta\sigma \qquad (34a)$$

$$\sin\sigma_n = \sin(\sigma_j + \Delta\sigma) \cong \sin\sigma_j + (\cos\sigma_j)\Delta\sigma \qquad (34b)$$

and, linearizing the logarithm, the above transcendental equation (33) becomes,

$$\left[\cos\eta[\cos\eta + (L/D)\sin\eta]\sin^2\sigma_j + \cos^2\sigma_j\right](1 + \sin\sigma_j)\Delta\sigma = 0 \qquad (35)$$

Assuming that $1 + \sin\sigma_j \neq 0$, and $\Delta\sigma \neq 0$, (35) becomes

$$\cos\eta[\cos\eta + (L/D)\sin\eta]\sin^2\sigma_j + \cos^2\sigma_j = 0 \qquad (36a)$$

From (29a),

$$\cos\sigma_j = \frac{A}{\tan\eta + L/D}\ ; \qquad A = m_j K_1 \qquad (36b)$$

Using (36b) in (36a),

$$[\tan\eta + L/D]\left[(L/D)\tan^2\eta + \{(L/D)^2 - A^2 - 1\}\tan\eta - L/D\right] \qquad (37)$$

Again, assuming $\tan\eta + L/D \neq 0$, we finally get a simplified form as,[11]

$$(L/D)\tan^2\eta + [(L/D)^2 - A^2 - 1]\tan\eta - L/D = 0 \qquad (38)$$

The implication of $\tan\eta + L/D = 0$ is that (a) $90^0 < \eta < 180^0$, or (b) $270^0 < \eta < 360^0$. The first condition implies that the thrust T will aid the drag force

instead of opposing it, and the second condition shows that the thrust T will oppose the lift instead of aiding it.

Summarizing, for bank angle control we have

$$\frac{d\psi}{dt} = K_3 \tan\sigma \tag{39a}$$

$$\frac{dm}{dt} = - K_2/\cos\eta \tag{39b}$$

The cruise condition is given by

$$\cos\sigma = mK_1/[\tan\eta + L/D] \tag{39c}$$

The sequence of solutions is

(i) Using initial masses m_j, and L/D, solve (38) for optimal thrust angle η.

(ii) Using η, m_j, and L/D, solve (39c) for σ_j.

(iii) Using η, and m_j, solve for new m from (39b).

(iv) Using the mass m, and η, solve (39a) or (31) for new ψ.

(v) Go to (ii), and repeat the steps.

(vi) Integration stops when m reaches the final m_n in (39b) and the corresponding maximum heading angle ψ_n is obtained from (39a).

Although (39) can be solved for either set of given values of (a) m_j and m_n or (b) ψ_j and ψ_n, the condition (38) requires m_j and m_n to determine the optimal η which is kept constant throughout the aerocruise mode. Hence, given the fuel consumption ($m_j - m_n$), we are trying to determine the maximum heading angle change.

V. AEROCRUISE MODE: THRUST CONTROL

Here, we keep the bank angle constant throughout and change the thrust magnitude and angle in order to achieve the desired heading change and hence the inclination.[12] For the sake of simplicity, we repeat the equations at cruise,

$$\frac{d\theta}{dt} = V\cos\psi/R \tag{40a}$$

$$\frac{dm}{dt} = -K_2/\cos\eta \tag{40b}$$

$$\frac{d\psi}{dt} = K_3\tan\sigma \tag{40c}$$

The cruise conditions are given by

$$T\cos\eta = D \tag{41a}$$

$$(T\sin\eta + L)\cos\sigma = m(g - V^2/R) \tag{41b}$$

Combining the two conditions,

$$\tan\eta = mK_1/\cos\sigma - L/D \tag{42}$$

For a constant altitude H, speed V, and given angle of attack α and bank angle σ, as the mass m changes, the thrust angle η follows (42). At the same time, the drag force D is to be kept constant as per (41a). Thus, in order to satisfy both the conditions (41), we need to adjust thrust magnitude T and angle η in such a way that $T\cos\eta$ is kept constant, and $T\sin\eta$ changes as per mass m. From (40), we see that the bank angle is kept constant throughout the cruise mode and hence the rate of change of heading angle is constant, whereas the mass flow rate is variable. This is in contrast to the bank angle control discussed in the last section.

Given a constant bank angle σ, the initial and final conditions m_j, ψ_j, m_n (or ψ_n), the sequence of solutions for the cruise flight with thrust control is first, solve the cruise condition equation (42) for η, second solve mass rate equation (40b) for m, and finally solve the heading angle equation (40c) for ψ. In the next section we try to find the optimal bank angle which should be kept constant throughout the cruise, to get maximum heading change.

Optimization of Heading Angle w.r.t. Bank Angle

Here, we are interested in finding the optimum bank angle so that the heading change is maximized. For this, we first solve (40)-(42) for the heading angle and then find the stationary value of ψ w.r.t. σ. Thus,

$$\psi_n = (I_{sp} g/V)\sin\sigma \ln\left[\frac{\sec\eta_j + \tan\eta_j}{\sec\eta_n + \tan\eta_n}\right] \tag{43a}$$

where,

$$\tan\eta_i = m_i K_1/\cos\sigma - L/D; \quad \sec^2\eta_i = 1 + \tan^2\eta_i; \quad i = j,\ n \tag{43b}$$

$$K_6 = (I_{sp}\ g/V)\sin\sigma \tag{43c}$$

Alternatively, (43a) can be used to find the mass m for a given ψ. Use of the stationary condition leads to

$$\cos^2\sigma \ln\left[\frac{\cos\eta_j(1 + \sin\eta_n)}{\cos\eta_n(1 + \sin\eta_j)}\right] + \sin^2\sigma\left[(\sin\eta_n - \sin\eta_j) + (L/D)(\cos\eta_n - \cos\eta_j)\right] = 0 \tag{44}$$

Considering only the first order approximations in the thrust angle η

$$\cos\eta_n = \cos(\eta_j + \Delta\eta) \cong \cos\eta_j - (\sin\eta_j)\Delta\eta \tag{45a}$$

$$\sin\eta_n = \sin(\eta_j + \Delta\eta) \cong \sin\eta_j + (\cos\eta_j)\Delta\eta \tag{45b}$$

and linearizing the logarithm, the transcendental equation (44) becomes

$$\left\{\cos^2\sigma + \sin^2\sigma\left[\frac{1 - (L/D)\tan\eta_j}{1 + \tan^2\eta_j}\right]\right\}[1 + \sin\eta_j]\Delta\eta = 0 \tag{46}$$

Assuming $1 + \sin\eta_j \neq 0$; and $\Delta\eta \neq 0$, (46) reduces to

$$\cos^2\sigma + \sin^2\sigma\left[\frac{1 - (L/D)\tan\eta_j}{1 + \tan^2\eta_j}\right] = 0 \tag{47}$$

Using

$$\tan\eta_j = A/\cos\sigma - L/D \tag{48}$$

in (47), we get a simplified quadratic equation in $\cos\sigma$ as

$$(L/D)A\cos^2\sigma - [(L/D)^2 + A^2 + 1]\cos\sigma + (L/D)A = 0 \tag{49}$$

It is interesting to note that the optimal conditions (38) and (49) for bank control and thrust control respectively, are interchangeable by the cruise condition (36b) or (48).

Summarizing, for thrust control we have

$$\frac{d\psi}{dt} = K_3\tan\sigma \tag{50a}$$

$$\frac{dm}{dt} = -K_2/\cos\eta \tag{50b}$$

The cruise conditions are given by

$$T\cos\eta = D \tag{50c}$$

$$\tan\eta = mK_1/\cos\sigma - L/D \tag{50d}$$

The sequence of solutions is

(i) Using initial mass m_j and L/D, solve (49) for optimal bank angle σ.

(ii) Using σ, m_j, and L/D, solve (50d) for η_j.

(iii) Using η_j, find the thrust T_j from (50c).

(iv) Using ψ_j, and σ, solve (50) for new ψ.

(v) Using η_j, and m_j, solve for new m from (50b) or (43).

(vi) Go to (ii), and repeat the steps.

(vii) Integration stops when m reaches the final m_n in (50b) and the corresponding maximum heading angle ψ_n is obtained from (50a).

Although (50) can be solved for either set of given values of (a) m_j and m_n or (b) ψ_j and ψ_n, the condition (49) requires m_j and m_n to determine the optimal σ which is kept constant throughout the aerocruise mode. Hence, given the fuel consumption ($m_j - m_n$), we are trying to determine the maximum heading angle change.

VI. ASCENT MODE

This is just a replica of the descent mode except for the change in the mass of the vehicle, and the boundary conditions. Thus, we go through the equations of motion, change the independent variable to flight path angle, and finally assume that there is no appreciable change in heading angle. Thus,

$$\frac{dH}{d\gamma} = 2m_n \exp(\beta H)\sin\gamma/\rho_0 SC_L \tag{51a}$$

$$\frac{dV}{d\gamma} = - C_D V/C_L \tag{51b}$$

The optimal control problem is posed as follows. Given initial conditions (or the conditions at the end of the cruise mode), and the conditions at the end of the ascent mode, find the optimal control law which maximizes the final velocity.[10] The performance index is given by

$$J = - V_f \tag{52}$$

The Hamiltonian for (51) and (52) is

$$\mathcal{H} = \lambda_H\left[2m_n \exp(\beta H)\sin\gamma/\rho_0 SC_L\right] + \lambda_v\left[- C_D V/C_L\right] \tag{53}$$

The adjoint equations are

$$d\lambda_H/d\gamma = -\lambda_H 2m_n \beta \exp(\beta H)\sin\gamma/\rho_0 SC_L \tag{54a}$$

$$d\lambda_v/d\gamma = \lambda_v C_D/C_L \tag{54b}$$

Solving the state (51) and costate (54) equations, we get

$$V\lambda_v = V_n \lambda_{vn} = \text{constant} \tag{55a}$$

$$\lambda_H \exp(\beta h) = \lambda_{Hn} \exp(\beta H_n) \tag{55b}$$

The boundary conditions for the adjoint variables are

$$\lambda_v(\gamma = \gamma_f) = \left.\frac{\partial J}{\partial V}\right|_{\gamma = \gamma_f} = -1 \tag{56a}$$

$$\lambda_H(\gamma = \gamma_f) = \left.\frac{\partial J}{\partial H}\right|_{\gamma = \gamma_f} = 0 \tag{56b}$$

From (55) and (56),

$$\lambda_H = 0 \tag{57}$$

With (57), the Hamiltonian (53) reduces to

$$\mathcal{H} = -\lambda_v V[C_{DO}/C_L + KC_L] \tag{58}$$

The optimal control is then given by

$$\frac{\partial \mathcal{H}}{\partial C_L} = 0 \tag{59}$$

leading to

$$C_{LO} = \sqrt{C_{DO}/K} = C_{LE} \tag{60}$$

where, C_{LE} is the lift coefficient for maximum lift-to-drag ratio $(L/D)_{max} = E = 1/2\sqrt{KC_{DO}}$. With optimal control (60) in (51), and noting that $\gamma_n = 0$, we solve for the velocity and altitude as

$$V(\gamma) = V_n \exp(-\gamma/E) \tag{61}$$

$$H = \ln\left[\exp(-\beta H_n) + \frac{2\beta m_n}{\rho_0 S C_{LO}}(\cos\gamma - 1)\right]^{-1/\beta} \tag{62a}$$

For small γ, (62a) reduces to

$$H = \ln\left[\exp(-\beta H_n) - \frac{\beta m_n}{\rho_0 S C_{LO}}\gamma^2\right]^{-1/\beta} \tag{62b}$$

At the end of the ascent mode, $\gamma = \gamma_f$ and $H = H_f$. Then (62) becomes

$$H_f = \ln\left[\exp(-\beta H_n) - \frac{\beta m_n}{\rho_0 S C_{LO}}\gamma_f^2\right]^{-1/\beta} \tag{63}$$

Using (19d) and (63) and noting that $H_e = H_f$ and $H_j = H_n$, we get

$$\gamma_f = -\gamma_e\sqrt{m_j/m_n} \tag{64}$$

The relation (64) shows that at the end of the atmospheric phase, the vehicle has to leave the atmosphere with a positive flight path angle higher in magnitude to that of the entry flight path angle. This is due to the fact that the mass m_n at the beginning of the ascent mode (or end of the cruise mode) is less than the mass m_j at the end of the descent mode (or beginning of the cruise mode).

VII. BOOST AND REORBIT PHASE

During the atmospheric flight, the vehicle performs the desired plane change and dissipates some energy due to atmospheric drag. Therefore, a second impulse is required to boost the vehicle back to orbital altitude. The vehicle exits the atmosphere at point F, with a velocity V_f and flight path angle γ_f. The additional impulse ΔV_b, required at the exit point F for boosting into an elliptic orbit with apogee radius R_c and the reorbit impulse ΔV_c required to insert the vehicle into a circular orbit at point C, are obtained by using the principle of conservation of energy and angular momentum at the exit point F, and the circularization point C. Thus, we have,[11]

$$(V_f + \Delta V_b)^2/2 - \mu/R_a = (V_c - \Delta V_c)^2/2 - \mu/R_c \tag{65}$$

$$(V_f + \Delta V_b)R_a\cos\gamma_f = R_c(V_c - \Delta V_c) \tag{66}$$

Solving for ΔV_b and ΔV_c from the above equations (65) and (66),

$$\Delta V_b = \sqrt{2\mu(1/R_a - 1/R_c)/\left[1 - (R_a/R_c)^2\cos^2\gamma_f\right]} - V_f \tag{67}$$

$$\Delta V_c = \sqrt{\mu/R_c} - \sqrt{2\mu(1/R_a - 1/R_c)/\left[(R_c/R_a)^2/\cos^2\gamma_f - 1\right]} \tag{68}$$

Finally, the vehicle is in a circular orbit (of radius R_c) moving with the velocity $V_c = \sqrt{\mu/R_c}$.

VIII. NUMERICAL DATA AND RESULTS

The following set of data is used for a typical orbital maneuvering research vehicle.[5-8]

Orbital Data

Altitude of HEO, H_d = 115,000 m

Altitude of LEO, H_c = 115,000 m

Altitude of atmospheric boundary, H_a = 110,000 m

Radius of Earth, R_E = 6,356,766 m

Acceleration due to gravity at sea level, g_0 = 9.80665 m/sec^2

Atmospheric density at sea level, ρ_0 = 1.225 kg/m^3

Gravitational constant of Earth, μ = 3.986x10^4 m^3/sec^2

Inverse atmospheric scale height, β = 1/7280 m^{-1}

Vehicle Data

Initial mass, m_j = 4760 kg

Propellent available for cruise, $(m_j - m_n)$ = 1810 kg

Final mass, m_n = 2950 kg

Aerodynamic reference area, S = 11.613 m^2

Specific fuel impulse, I_{sp} = 290 sec

The aerodynamic characteristics are described in terms of the angle of attack α as

$$C_L = -2.068686996\alpha^3 + 2.943200144\alpha^2 + 0.080347684\alpha + 0.031320026 \qquad (69a)$$

$$C_D = 0.267339707\alpha^3 + 1.814473159\alpha^2 - 0.389985867\alpha + 0.068372034 \qquad (69b)$$

Fig. 4 shows the variations of the lift and drag coefficients C_L, and C_D and Fig. 5 shows the variations of the lift-to-drag ratio E, and the aeropropulsive efficiency E_p as a function of the angle of attack α. The maximum lift-to-drag ratio of 2.3149 occurs at the angle of attack of 13 degrees.

Deorbit Phase

Initially, the vehicle is at a HEO altitude H_d of 115 km orbiting with a circular velocity V_d of 7847.97 m/sec. A deorbit impulse ΔV_d of 518.99 m/sec puts the vehicle in an elliptic orbit to intersect the atmospheric boundary at an altitude H_a of 110 km. At the atmospheric entry point, the velocity V_e is 7334.17 m/sec and the flight path angle γ_e is -0.77 deg.

Atmospheric Phase: Deorbit Mode

During the descent mode of atmospheric phase, the vehicle descends from an altitude H_a of 110,000 m at a velocity V_e of 7334.17 m/sec to a cruise altitude H_j of 72,521 m and the cruise velocity V_j of 7291.17 m/sec according to relations (18) and (19). During this time, the vehicle is maintained at an angle of attack of 13 degrees corresponding to the lift given by (17) for maximum lift-to-drag ratio. The time solutions of altitude, velocity, and flight path angle for the descent mode are shown in Fig. 6. The time taken for descent mode is found to be 494 seconds.

Cruise Mode: Bank Angle Control

The cruise mode is analyzed using bank angle control or thrust control. With bank angle control, for the same fuel consumption and a given L/D (or angle of attack α), the optimum thrust angle as obtained from (38) is represented in Fig. 7. With this optimum thrust angle, the corresponding heading angle is obtained from (32) and is shown in Fig. 8. It is seen that at these constant cruising conditions (of altitude of 72521 m, velocity of 7291.7 m/sec, and thrust of 6108.9 Nw), the maximum heading and hence maximum inclination of 18.56 degrees is achieved with a thrust angle of 44.72 degrees and at a higher angle of attack of 24 degrees rather than at the angle of

attack of 13 degrees corresponding to maximum *L/D*.[5-8] Corresponding to the maximum inclination of 18.56 degrees, the time solutions for mass, bank angle, and heading angle are shown in Fig. 9, where the total time taken for the cruise mode is 830 seconds.

Cruise Mode: Thrust Control

With thrust control, for the same fuel consumption and a given *L/D* (or angle of attack α), the optimum bank angle as obtained from (49) is shown in Fig. 10. With this optimum bank angle, the corresponding heading angle is obtained from (43) and is shown in Fig. 11. It is seen that at these cruising conditions, the maximum heading angle of 17.7 degrees is achieved with a bank angle of 51.9 degrees and at a higher angle of attack of 20 degrees rather than at the angle of attack of 13 degrees corresponding to maximum *L/D*. Corresponding to the maximum heading angle of 17.7 degrees, the time solutions for mass, thrust, thrust angle, and heading angle are shown in Fig. 12, where the total time taken for cruise mode is 1345 seconds.

The comparison of maximum heading angle as a function of angle of attack for both the control strategies shown in Fig. 13, indicates the superiority of bank control over thrust control. It is to be noted that the heading achieved depends on the type of control used, cruise conditions, and the angle of attack.

Atmospheric Phase: Ascent Mode

At the end of cruise mode, the vehicle ascends to the atmospheric boundary with a constant angle of attack of 13 degrees corresponding to maximum lift-to-drag ratio as given by (60). At the end of the ascent mode, the exit velocity V_f is 7238.1 m/sec, the flight path angle γ_f as given by (64) is 0.9781 deg. The time solutions are shown in Fig. 14.

For the atmospheric phase with bank angle control, the total solutions for altitude, velocity, flight path angle, heading angle, and heating rate are shown in Fig. 15. Similarly, total solutions for thrust control are shown in Fig. 16. The heating rate is computed from[5]

$$\dot{Q} = 3.08 \times 10^{-4} \rho_k^{1/2} V_k^{3.08} \quad \text{Watts/cm}^2 \tag{70}$$

where, ρ_k is expressed in kg/km^3, and V_k is expressed in km/sec.

Reorbit Phase

At the end of the atmospheric phase, a boost impulse ΔV_b of 380 m/sec is executed to bring the vehicle to its original altitude H_c of 110 km. At this time, once again a circularizing impulse ΔV_c of 247.97 m/sec is imparted to finally put the vehicle in circular orbit.

IX. CONCLUDING REMARKS

We have addressed the synergistic plane change problem in connection with orbital transfer employing aeroassist technology. The mission involved transfer from high Earth orbit to low Earth orbit with plane change being performed within the atmosphere. The complete mission consisted of a deorbit phase, an atmospheric phase, and finally a reorbit phase. The atmospheric maneuver was composed of an entry mode, a cruise mode, and finally an exit mode. The descent and ascent modes have been analyzed using flight path angle as an independent variable for maximizing the cruise and exit velocities with a constraint on the minimum cruise altitude. During the cruise mode, constant altitude and velocity were maintained by means of bank angle control with constant thrust or thrust control with constant bank angle. Conditions have been obtained for maximizing the heading angle. Under given cruising conditions, the maximum heading angle has been achieved with an angle of attack higher than that corresponding to the maximum lift-to-drag ratio. Comparison between the two control strategies has shown the superiority of bank control over thrust control in terms of the maximum achievable heading angle.

Acknowledgements

This research work was supported by the grant NAG1-736 from Spacecraft Control Branch, NASA Langley Research Center, Hampton, Virginia.

X. REFERENCES

1. Walberg, G. D., "A Survey of Aeroassisted Orbital Transfer," J. Spacecraft, 22, pp. 3-18, Jan.-Feb. 1985.

2. Nyland, F. S., "Considerations of applying continuous thrust during synergistic plane change", AAS 68-121, AAS/AIAA Astrodynamic Specialists Conference, Jackson, Wyoming, Sept. 1968.

3. Cuadra, E., and Arthur, P. D., "Orbit plane change by external burning aerocruise", J. Spacecraft & Rockets, 3, 347-352, March 1966.

4. Clauss, J. S. Jr., and Yeatman, R. D., "Effect of heating restraints on aeroglide and aerocruise synergistic maneuver performance", J. Spacecraft and Rockets, 4, 1107-1109, Aug. 1967.

5. Ikawa, H., and Rudiger, T. F., "Synergistic maneuvering of a winged spacecraft for orbital plane change", J. Spacecraft & Rockets, 19, 513-520, Nov.-Dec., 1982.

6. Cervisi, R. T., "Analytical solutions of a cruising plane change maneuver", J. Spacecraft & Rockets, 22, 134-140, Mar.-April 1985.

7. Blissit, J. A. Jr., "An adaptive guidance algorithm for an aerodynamically assisted orbital plane change maneuver", M.S. Thesis, Draper Labs., Cambridge, MA, June 1986.

8. Mease, K. D., Lee, J. Y., and Vinh, N.-X., "Orbital changes during hypersonic aerocruise", The J. Astro. Sciences, 36, 103-137, Jan.-June 1988.

9. Marec, J. P., Optimal Space Trajectories, Elsevier Scientific Publishing Company, Amsterdam, 1979.

10. Vinh, N.-X., Optimal Trajectories in Atmospheric Flight, Elsevier Scientific Publishing Co., Amsterdam, 1981.

11. Beiner, L., "A simplified three-dimensional altitude constrained skip maneuver for maximum orbit plane change", Israel J. of Technology, 13, 82-88, May 1975.

12. Bell, R. N., and Hankey, W. L., Jr., "Applications fo aerodynamic lift in accomplishing orbital plane change", Air Force Systems Command, Wright-Patterson Air Force BAse, Ohio, ASD-TDR-63, 693, Sept. 1963.

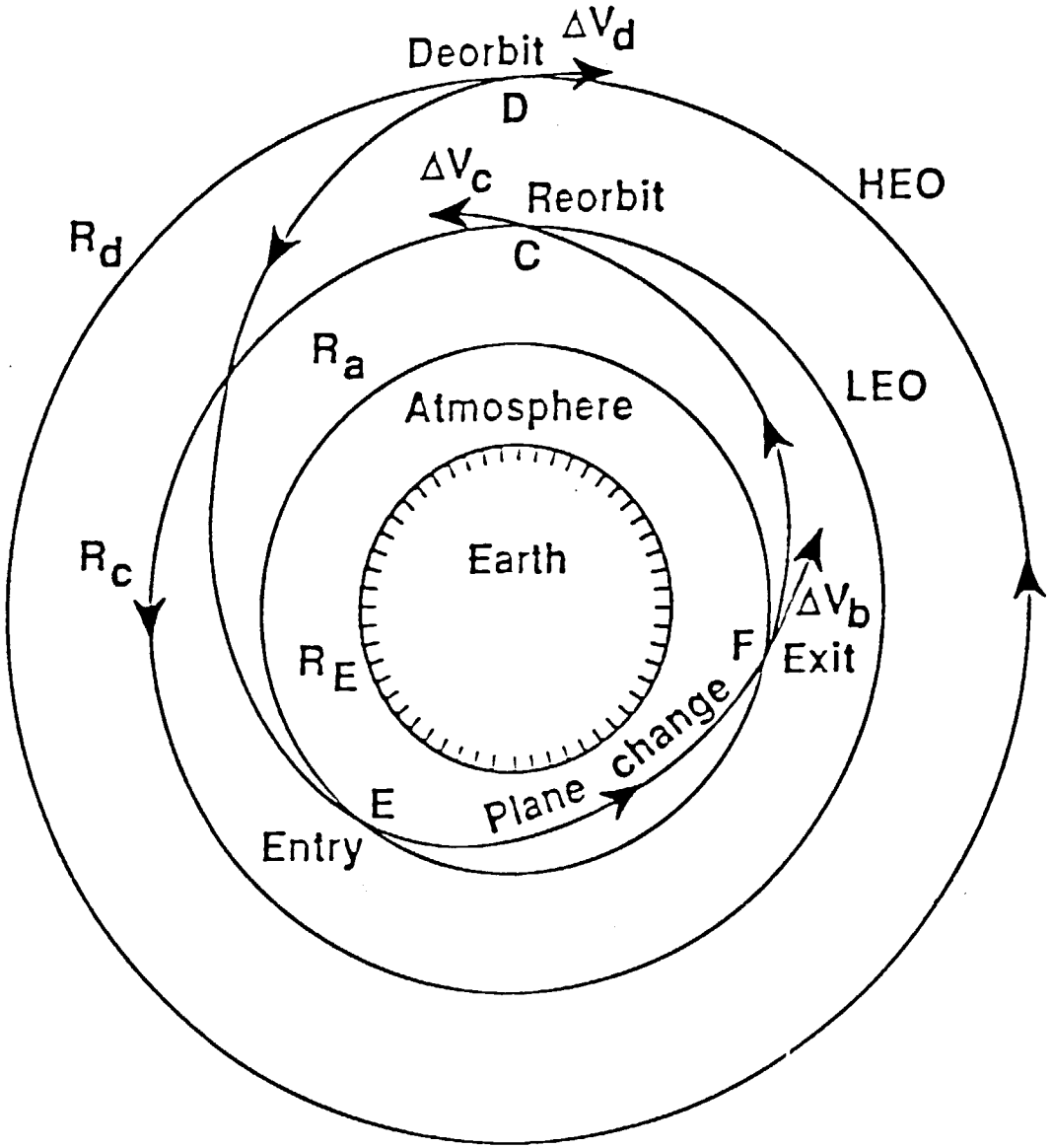


Fig. 1. Aeroassisted Orbital Transfer Mission

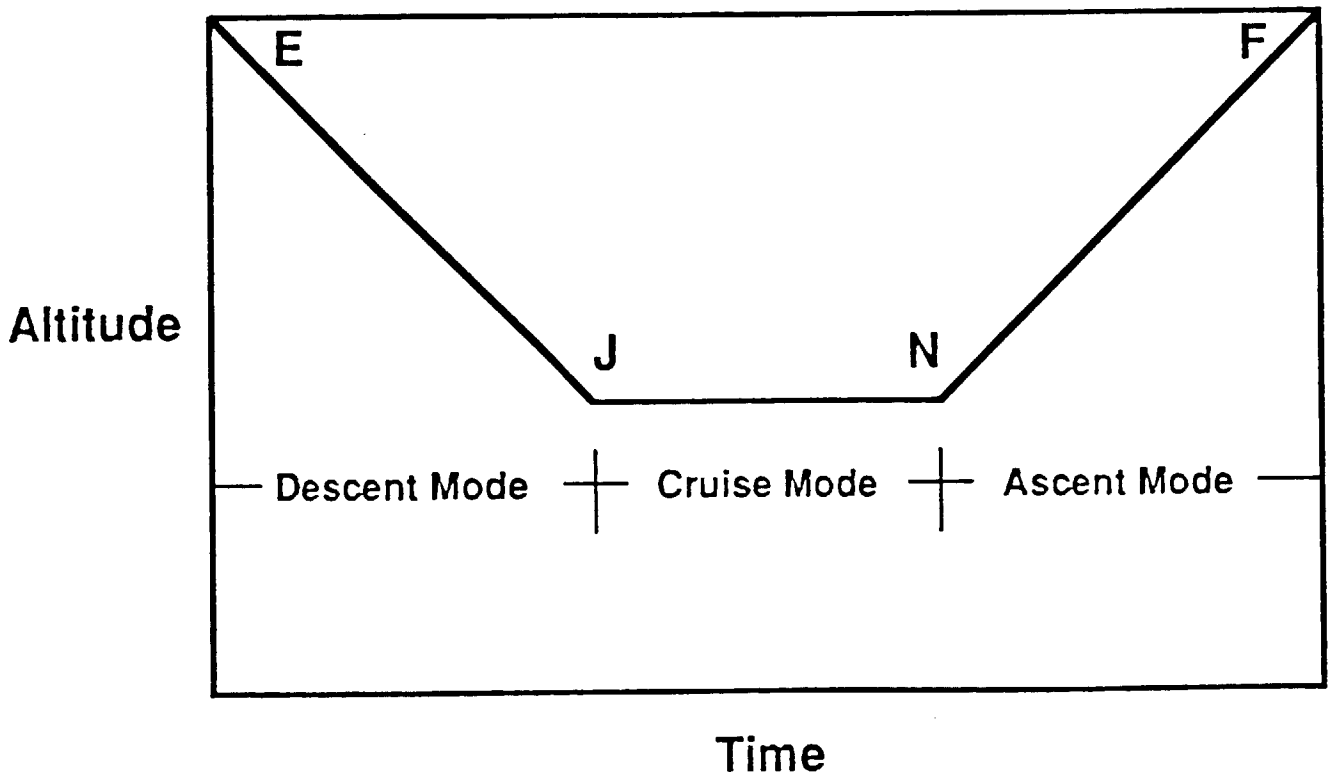


Fig. 2. Atmospheric Phase

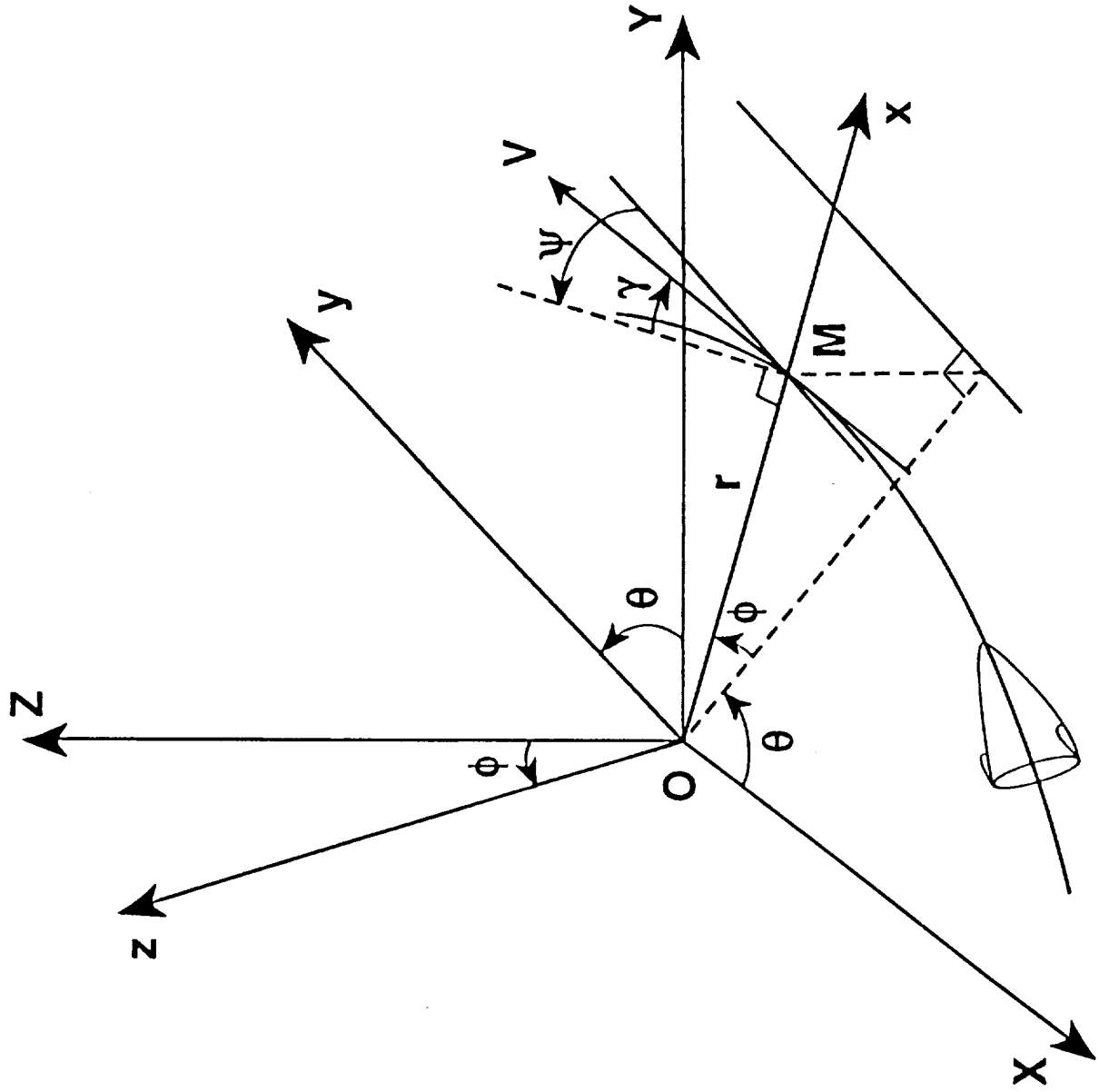


Fig. 3. Coordinate System

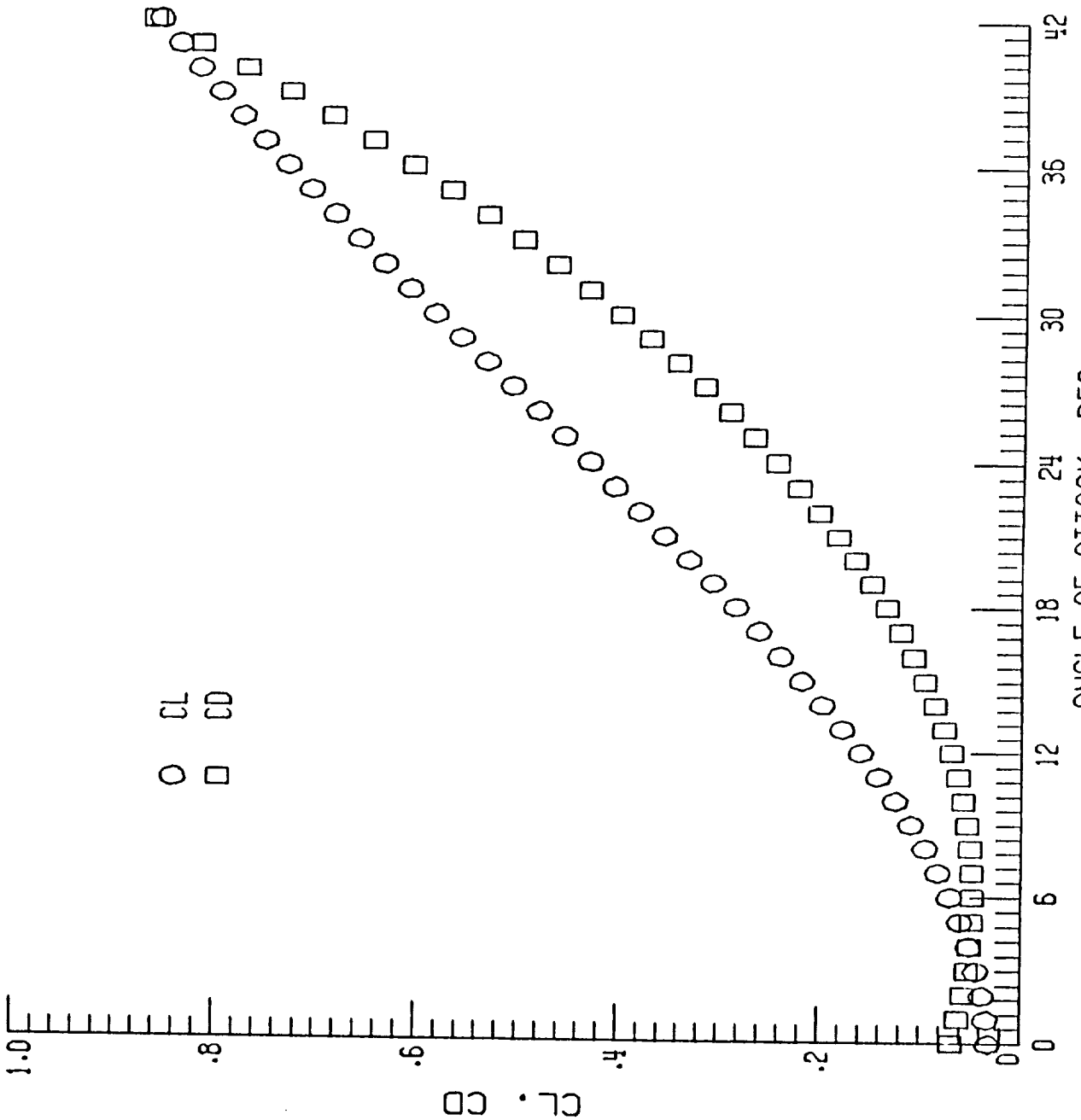


Fig. 4. Lift and Drag Coefficients

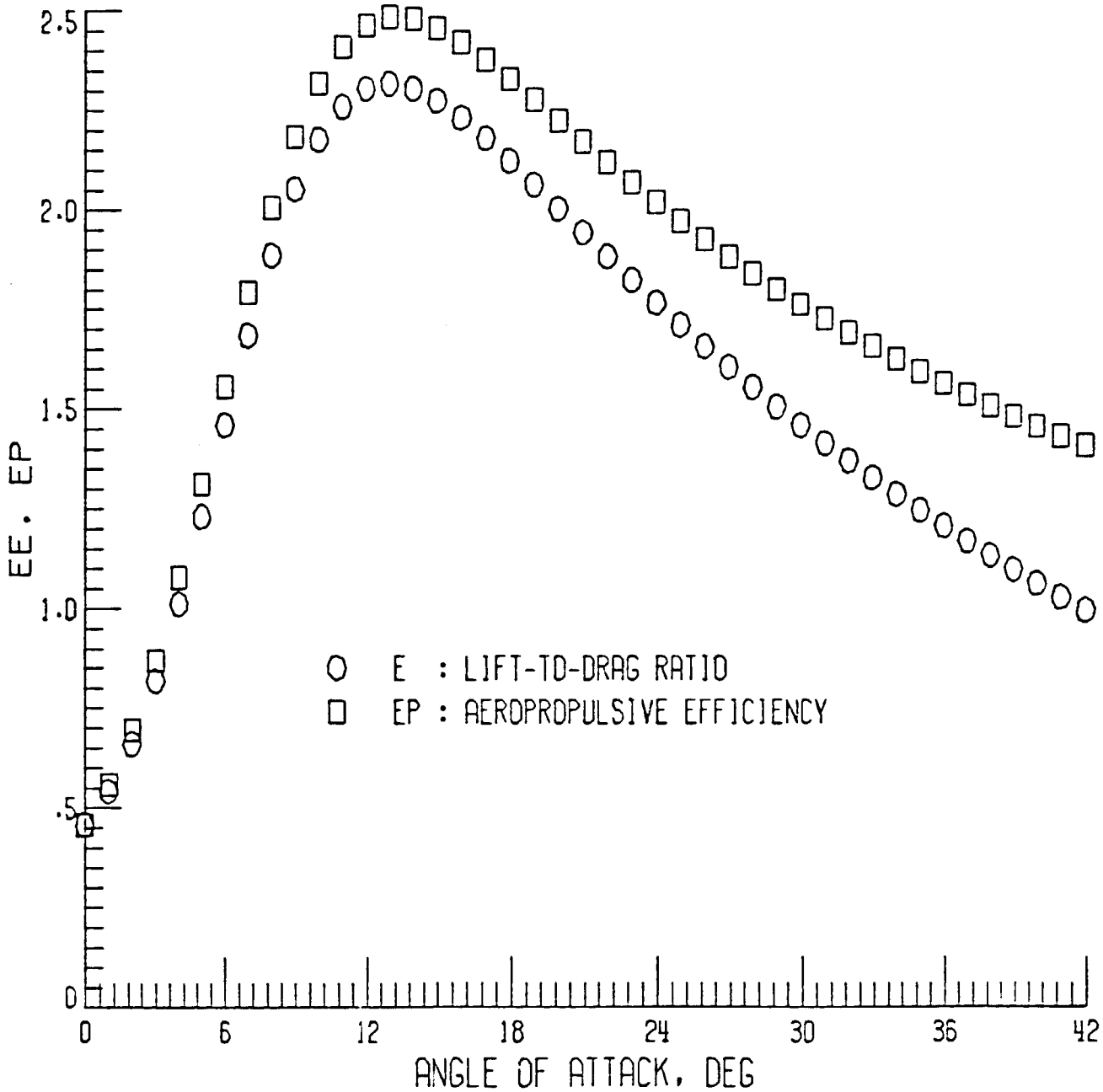


Fig. 5. Lift-to-Drag Ratio and Aeropropulsive Efficiency

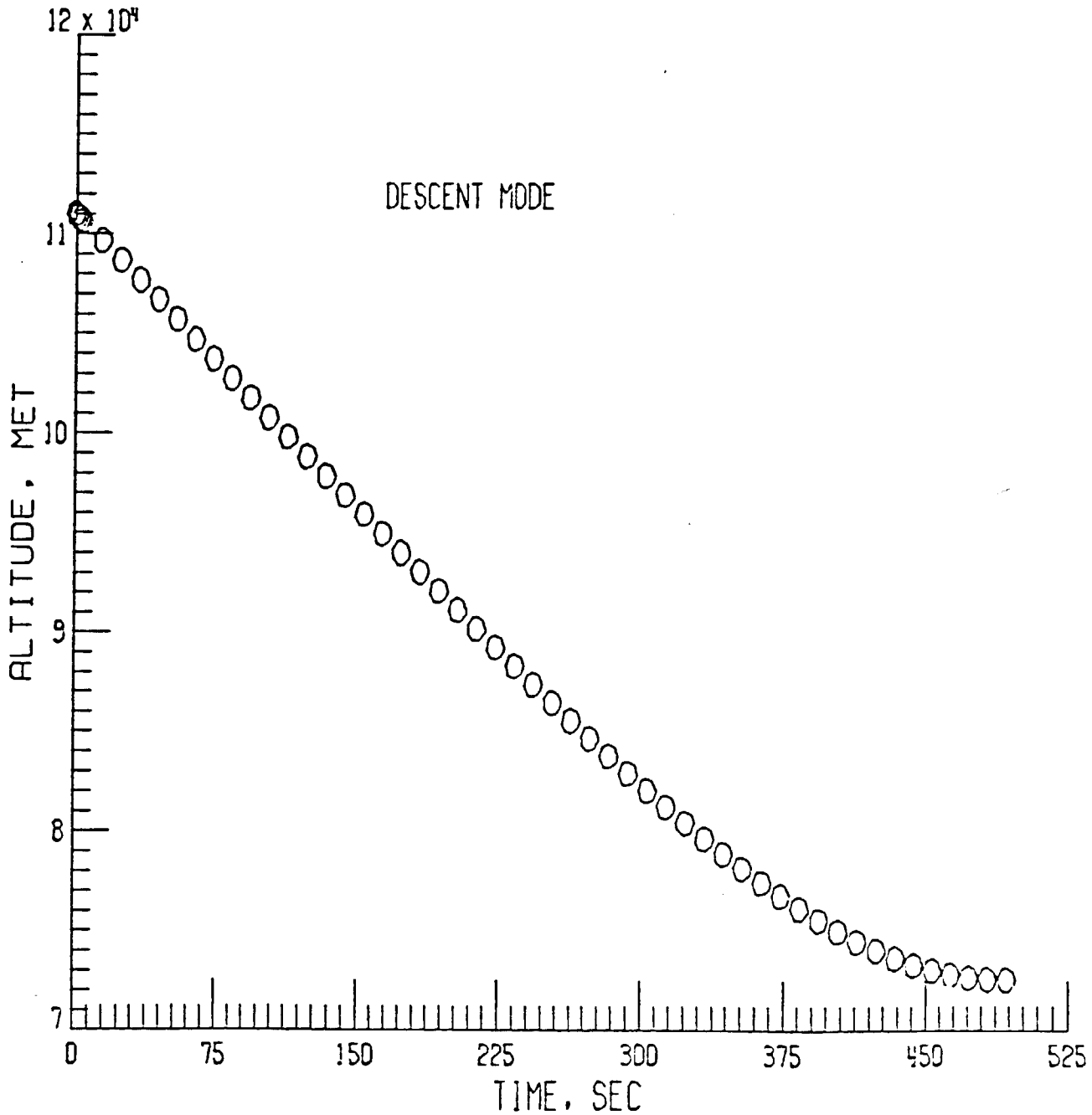


Fig. 6(a). Altitude as a Function of Time during Descent Mode

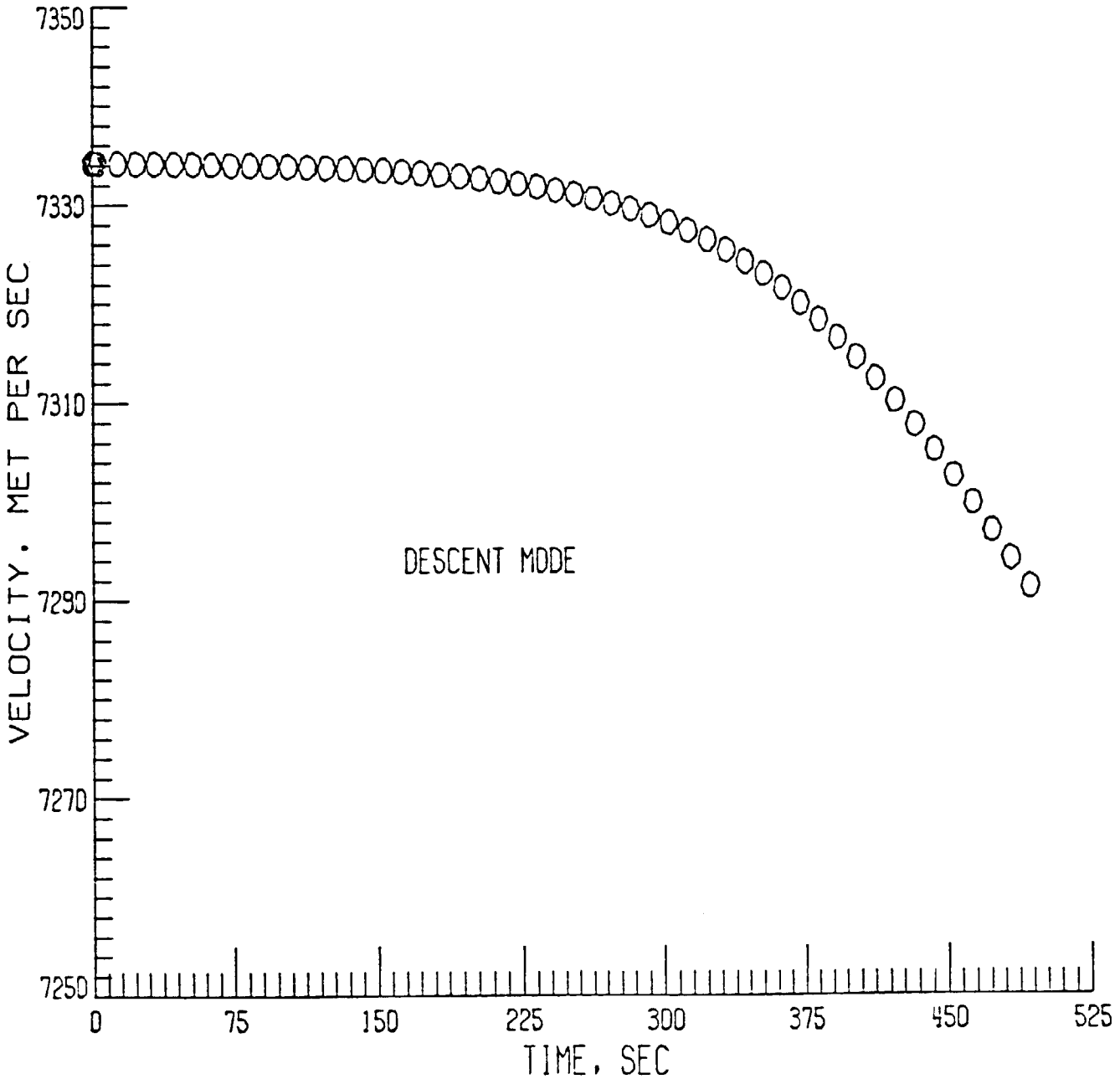


Fig. 6(b). Velocity as a Function of Time during Descent Mode

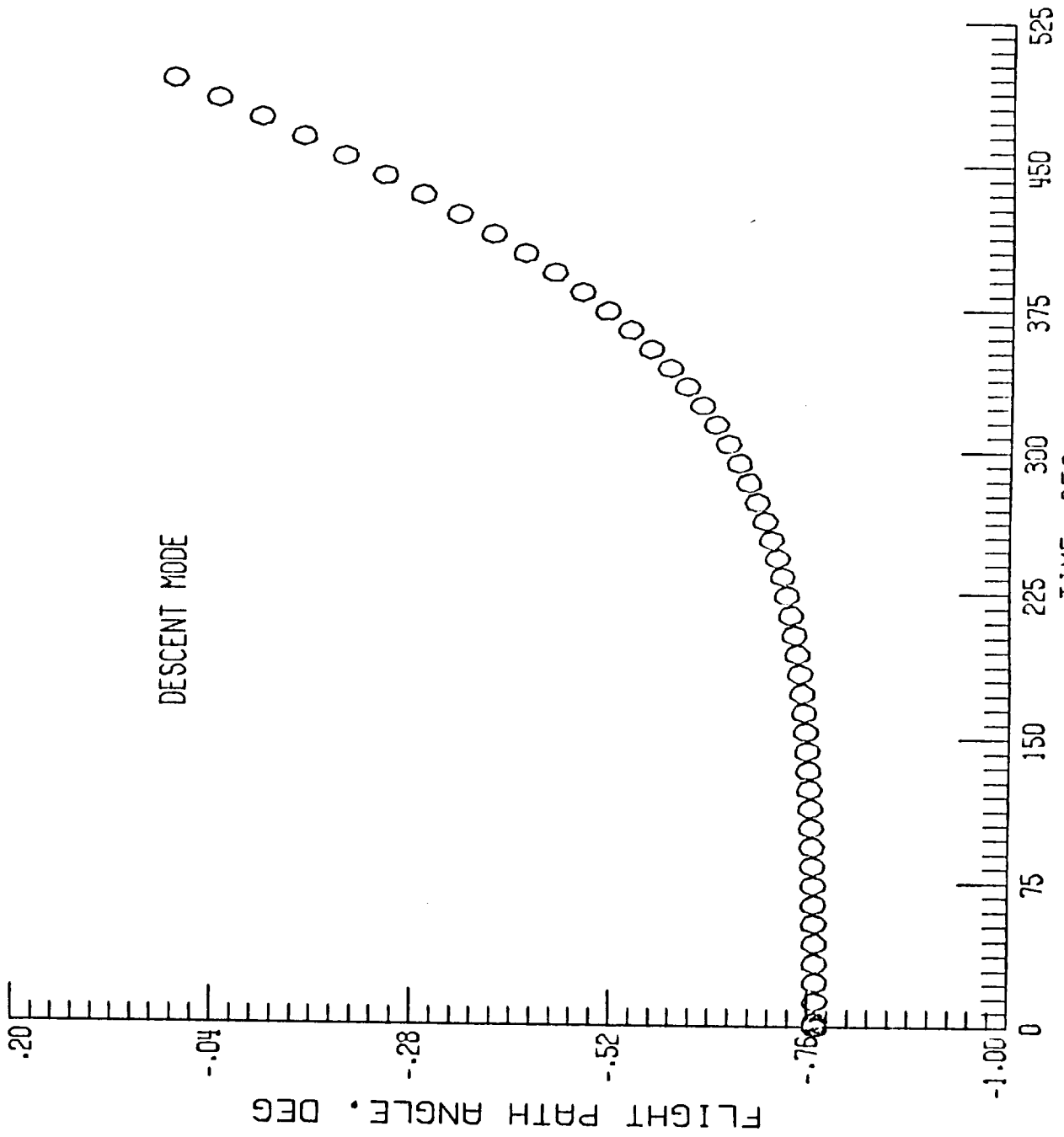


Fig. 6(c). Flight Path Angle as a Function of Time During Descent Mode

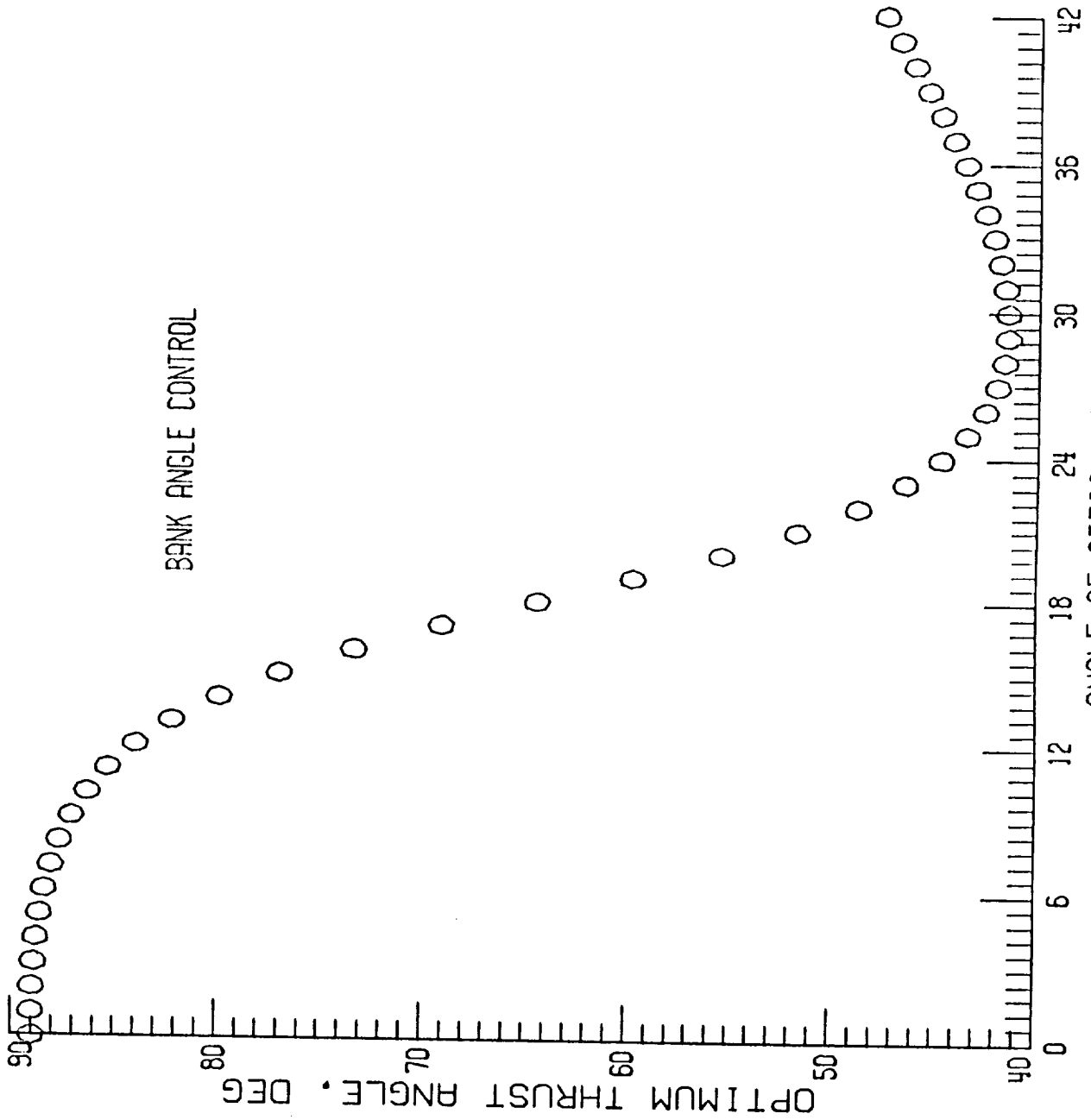


Fig. 7. Optimum Thrust Angle as a Function of Angle of Attack

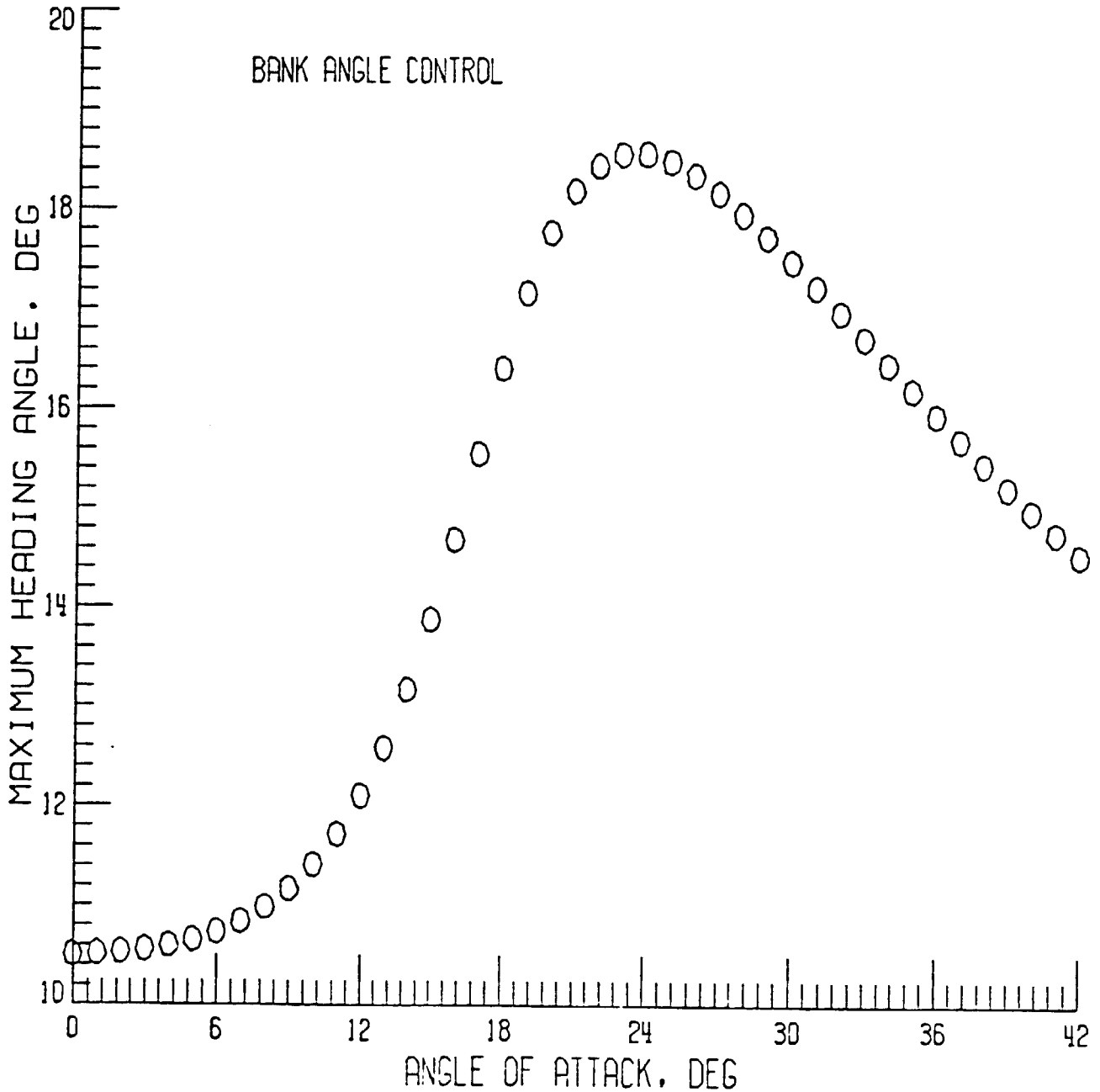


Fig. 8. Maximum Heading Angle as a Function of Angle of Attack

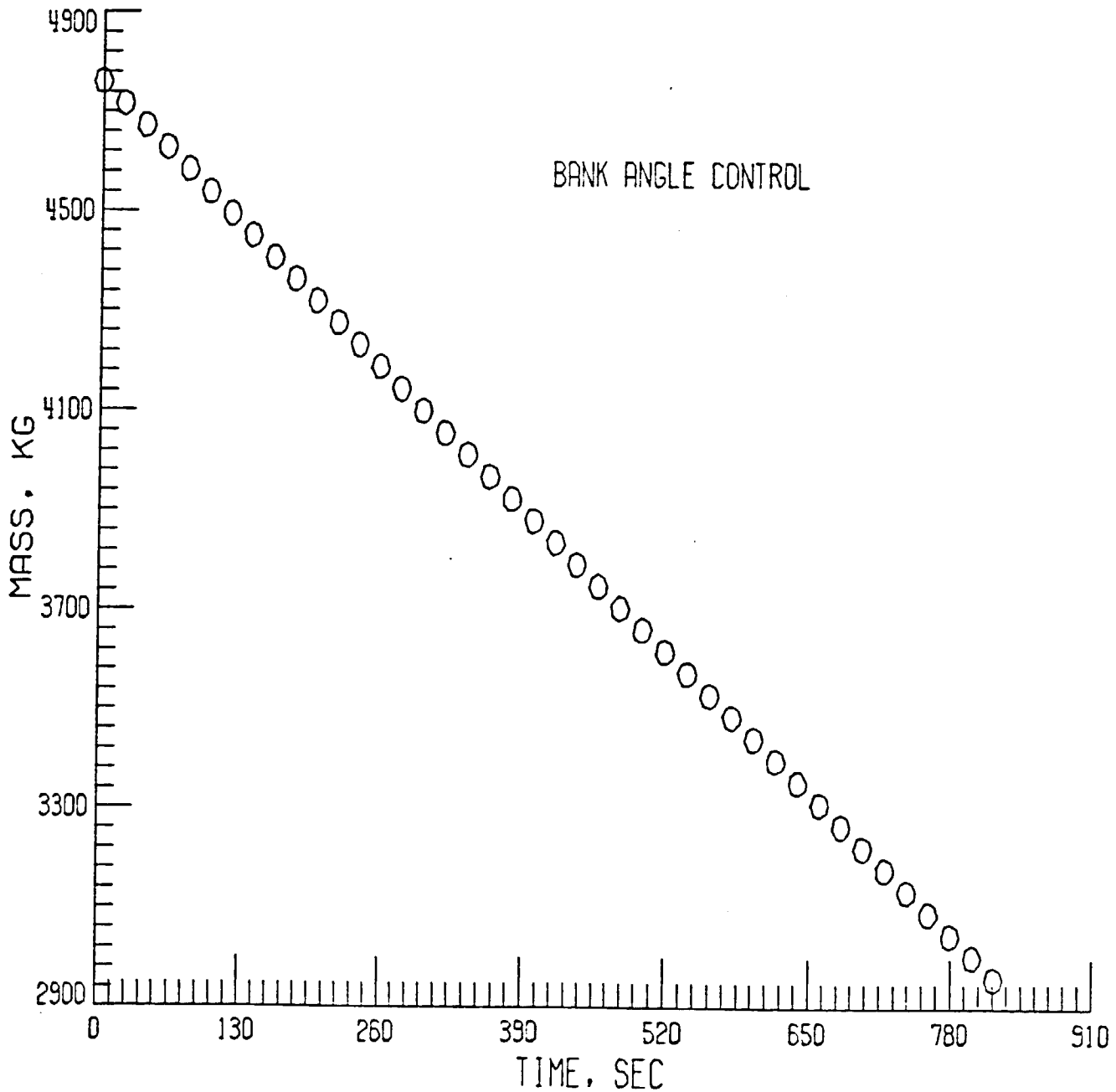


Fig. 9(a). Mass as a Function of Time with Bank Angle Control

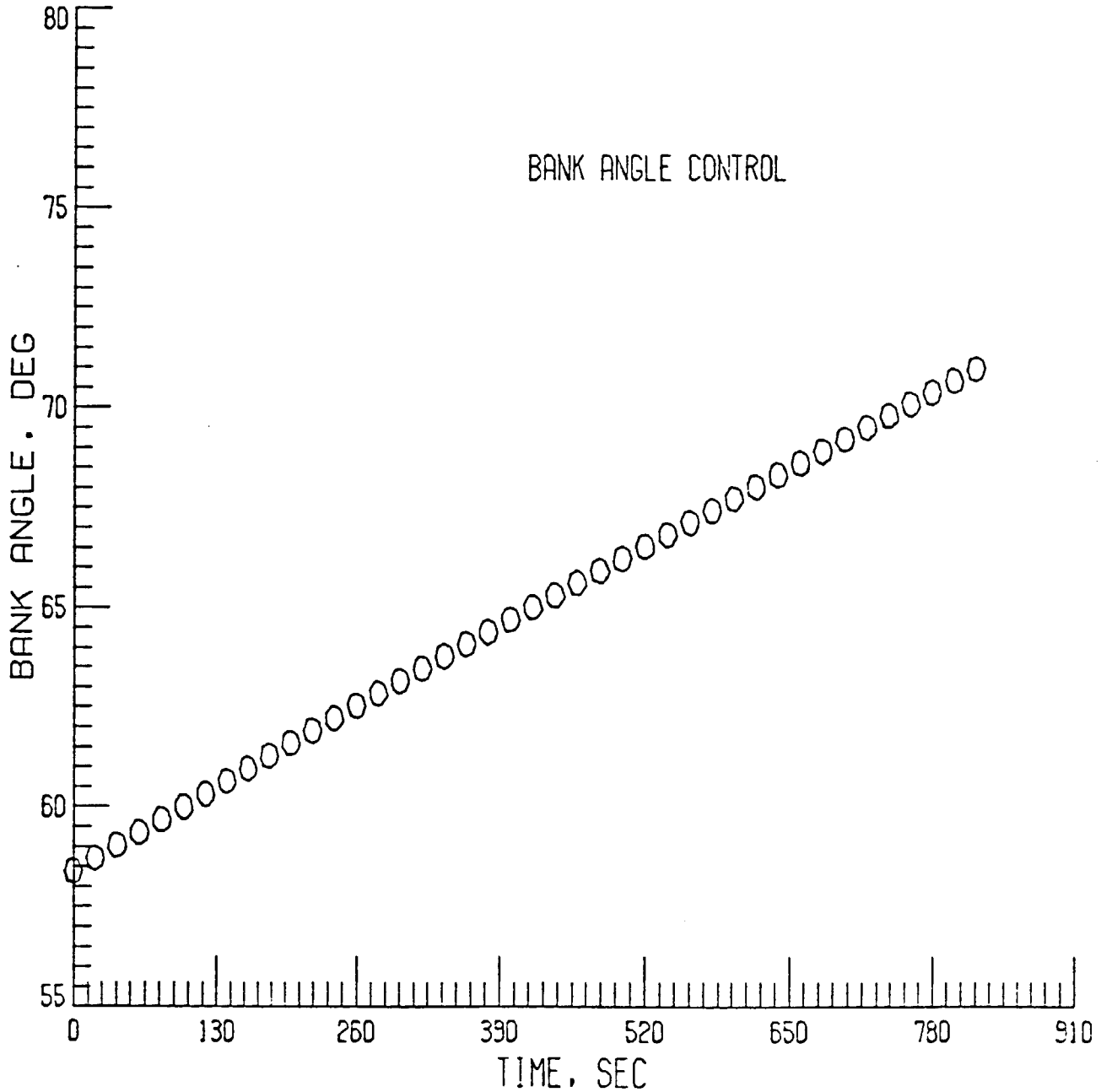


Fig. 9(b). Bank Angle as a Function of Time with Bank Angle Control

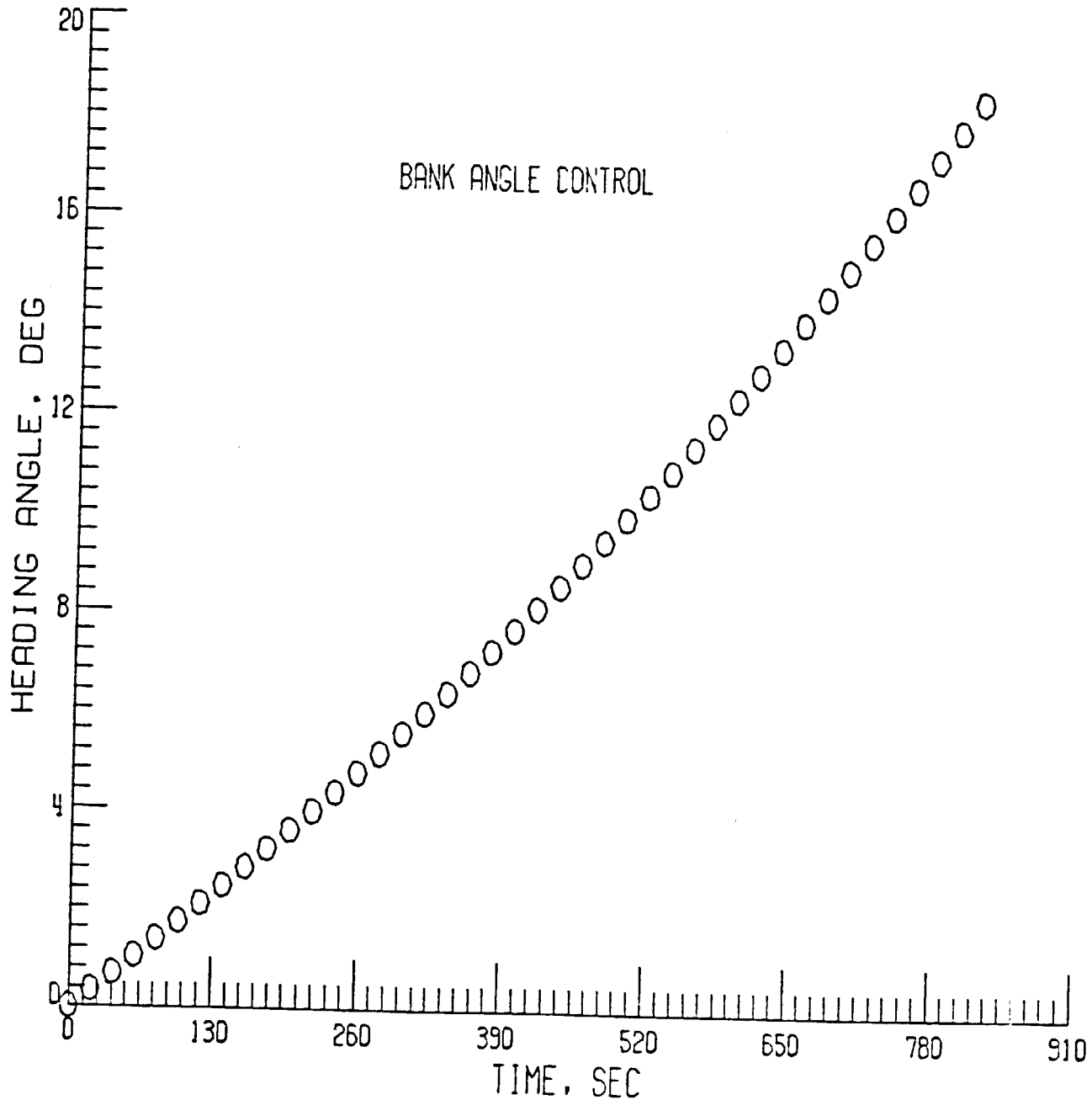


Fig. 9(c). Heading Angle as a Function of Time with Bank Angle Control

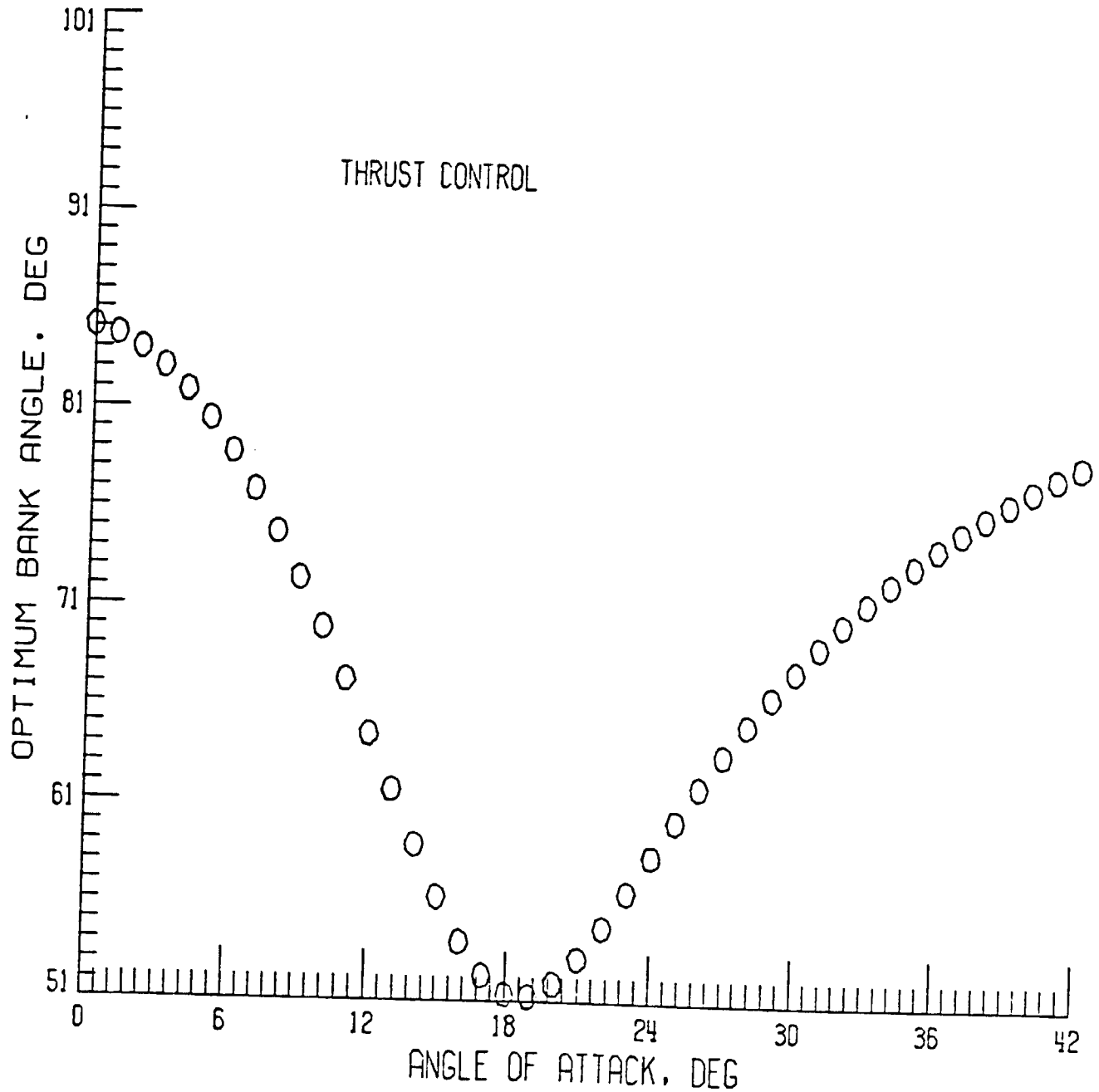


Fig. 10. Optimum Bank Angle as a Function of Angle of Attack

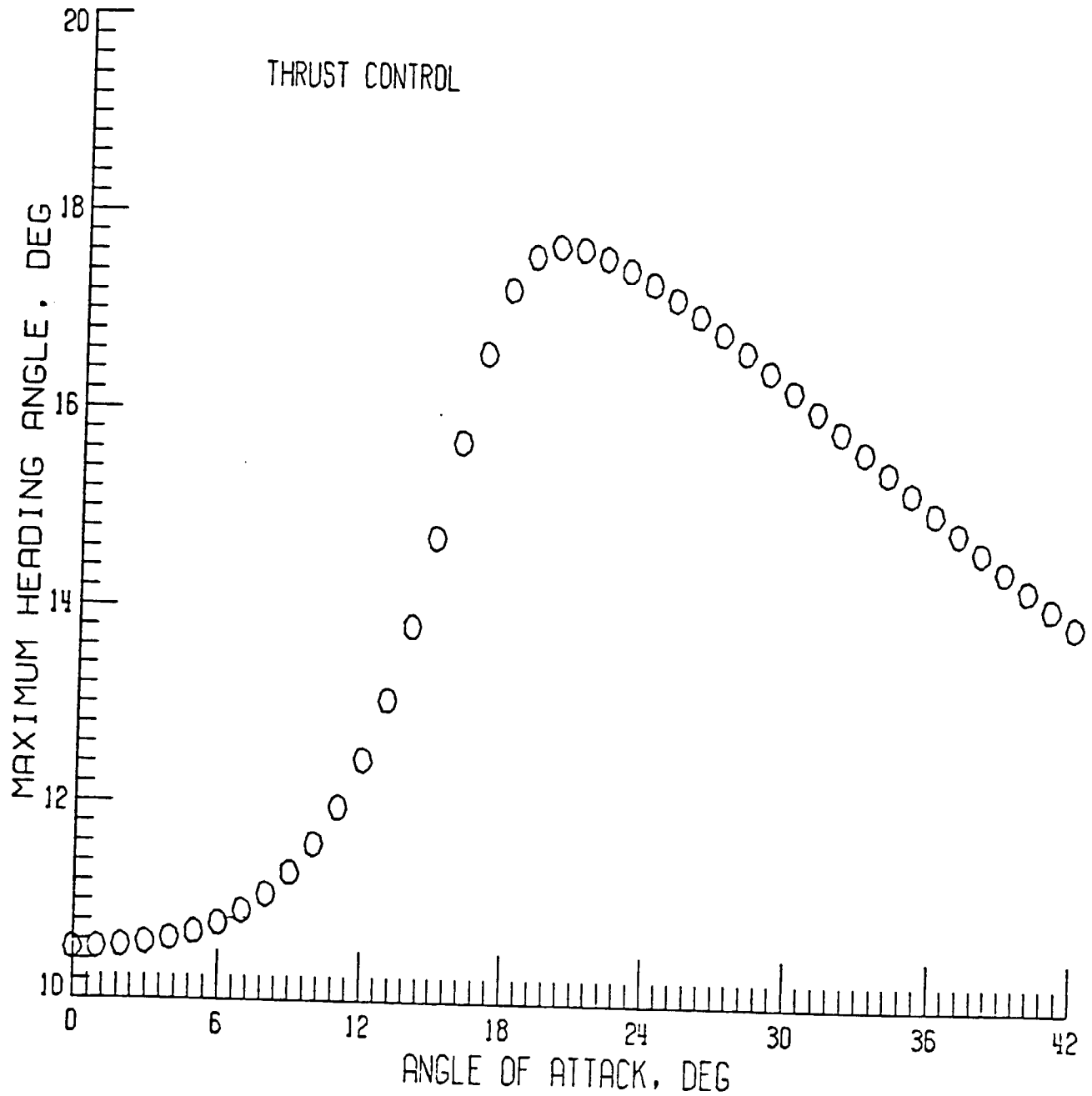


Fig. 11. Maximum Heading Angle as a Function of Angle of Attack

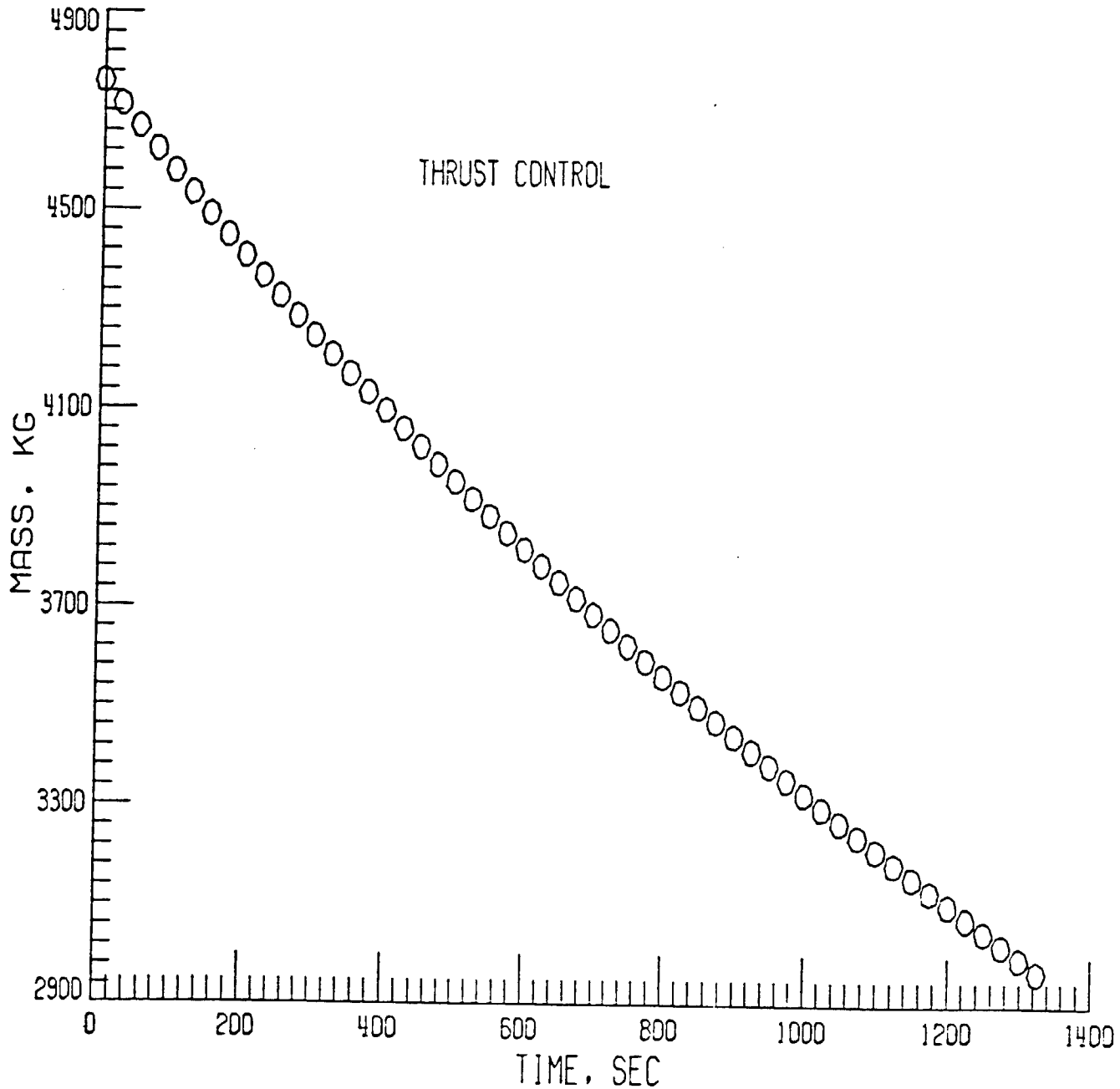


Fig. 12(a). Mass as a Function of Time with Thrust Control

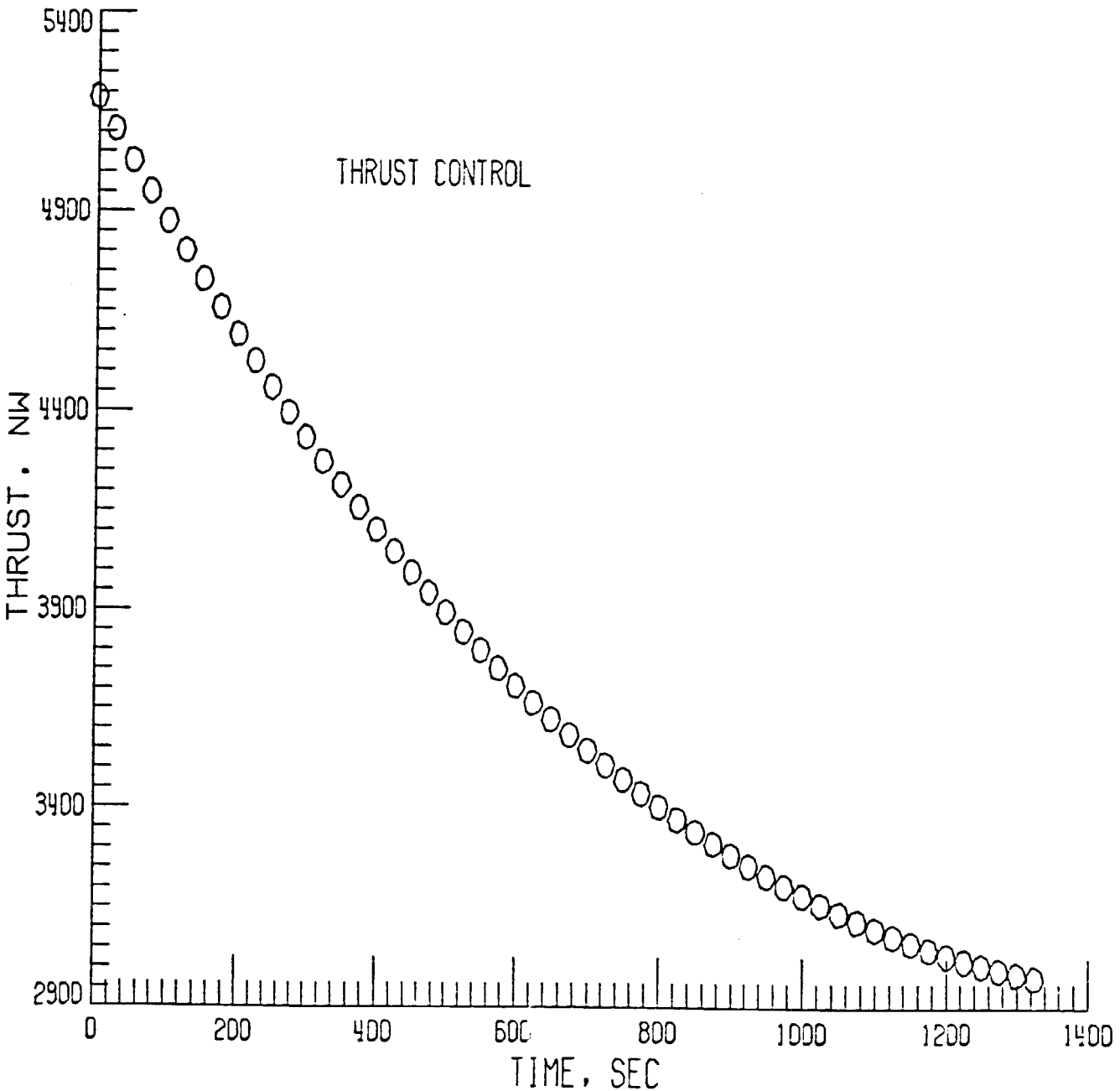


Fig. 12(b). Thrust as a Function of Time with Thrust Control

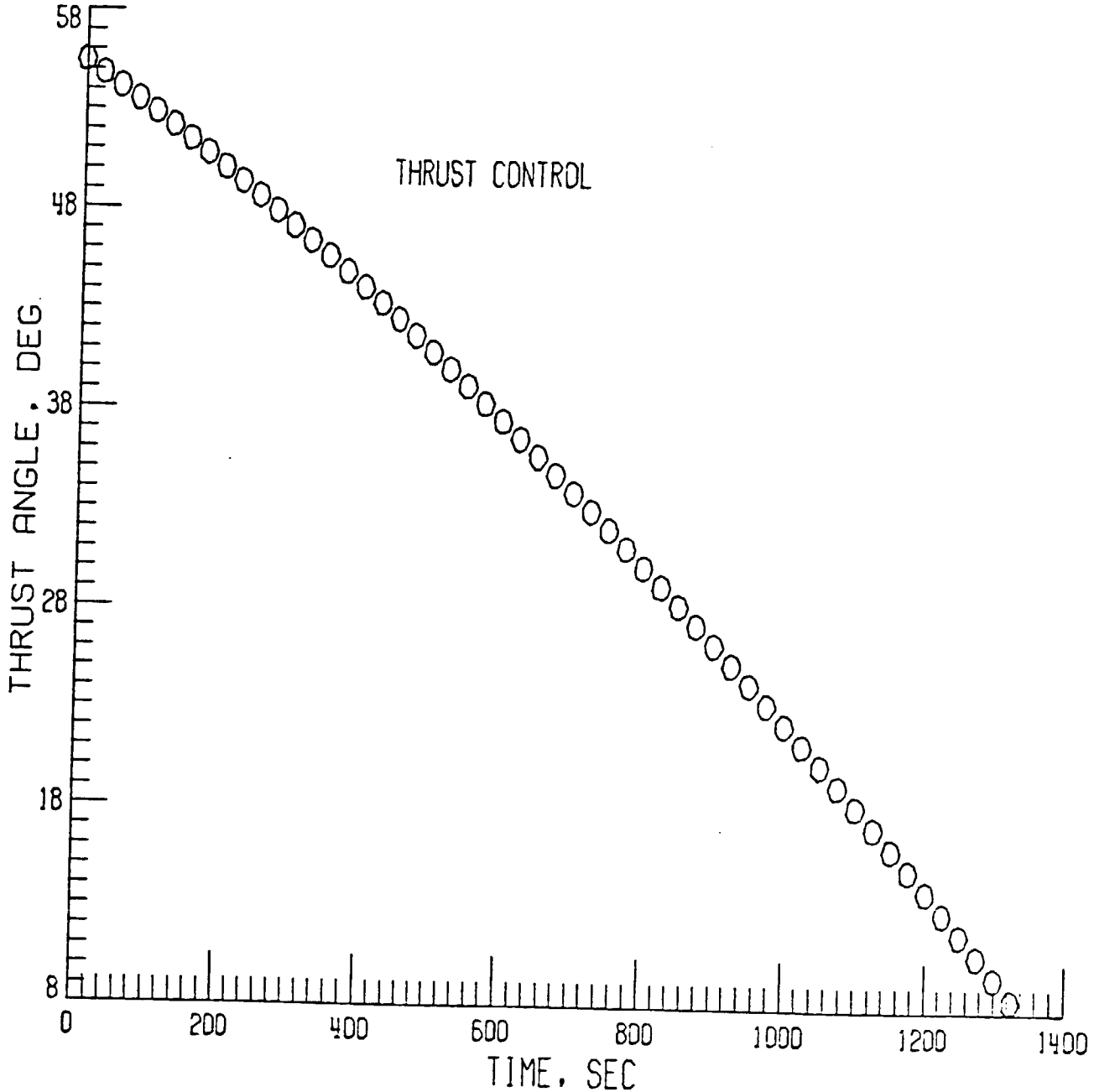


Fig. 12(c). Thrust Angle as a Function of Time with Thrust Control

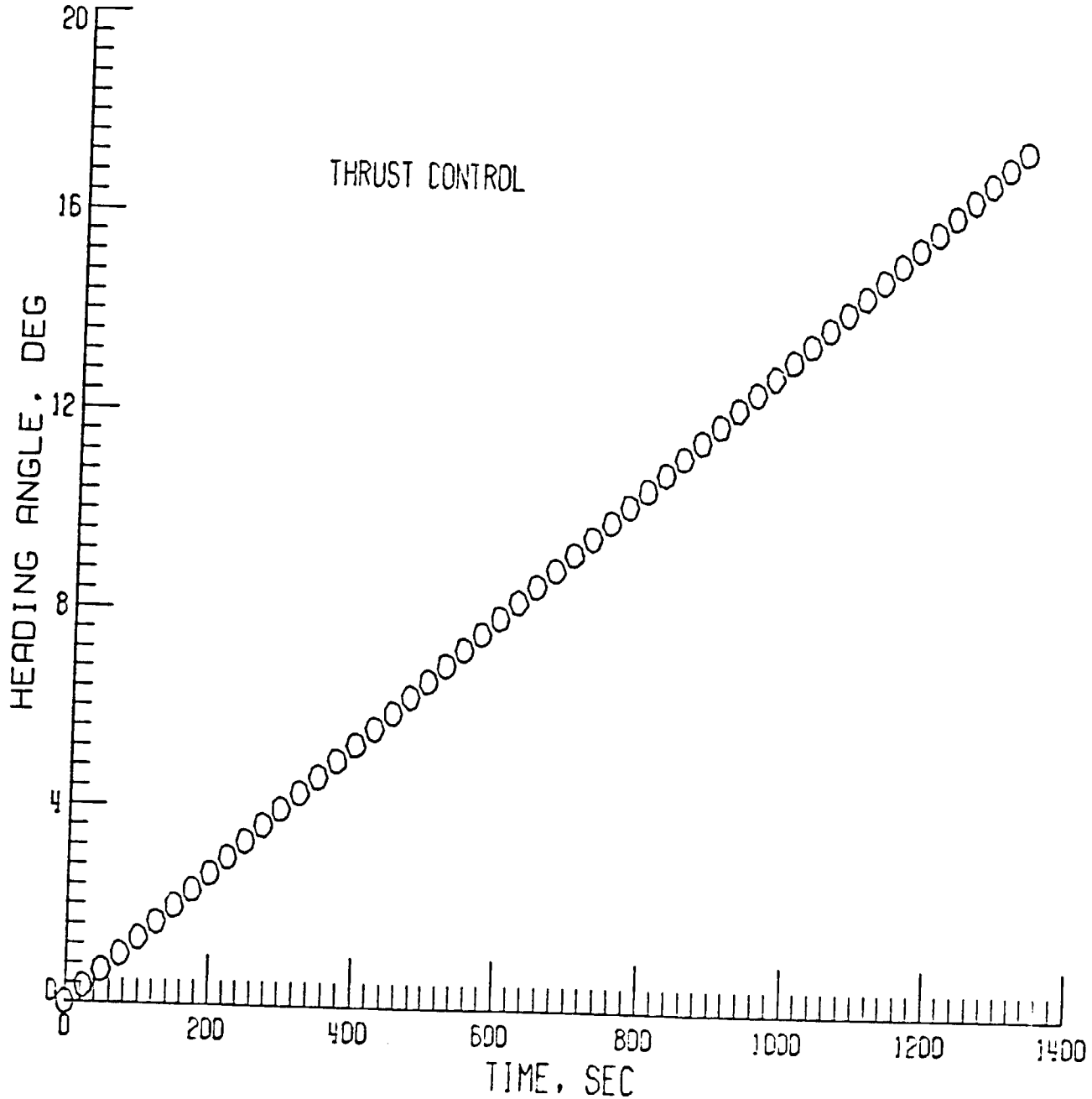


Fig. 12(d). Heading Angle as a Function of Time with Thrust Control

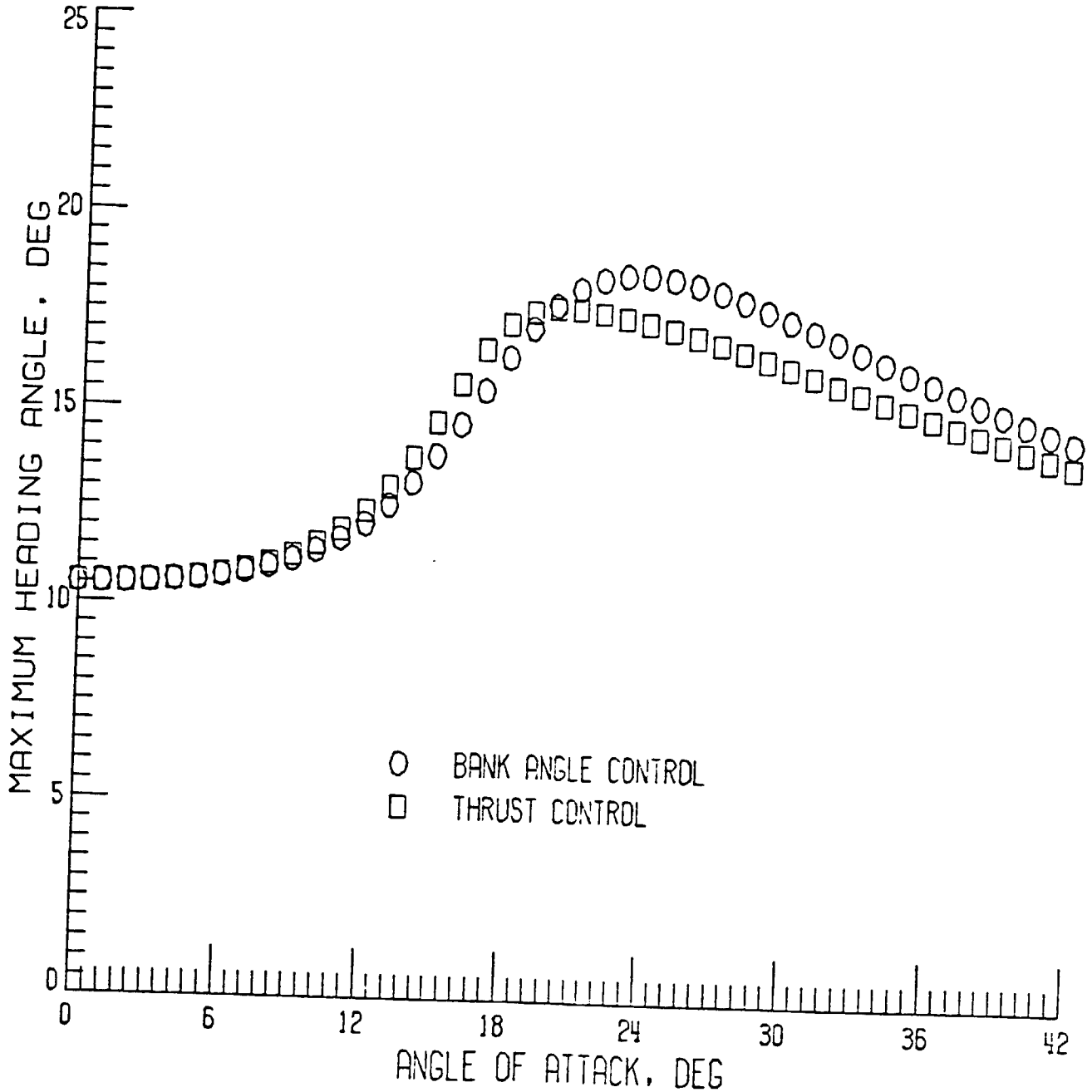


Fig. 13. Maximum Heading Angle as a Function of Angle of Attack

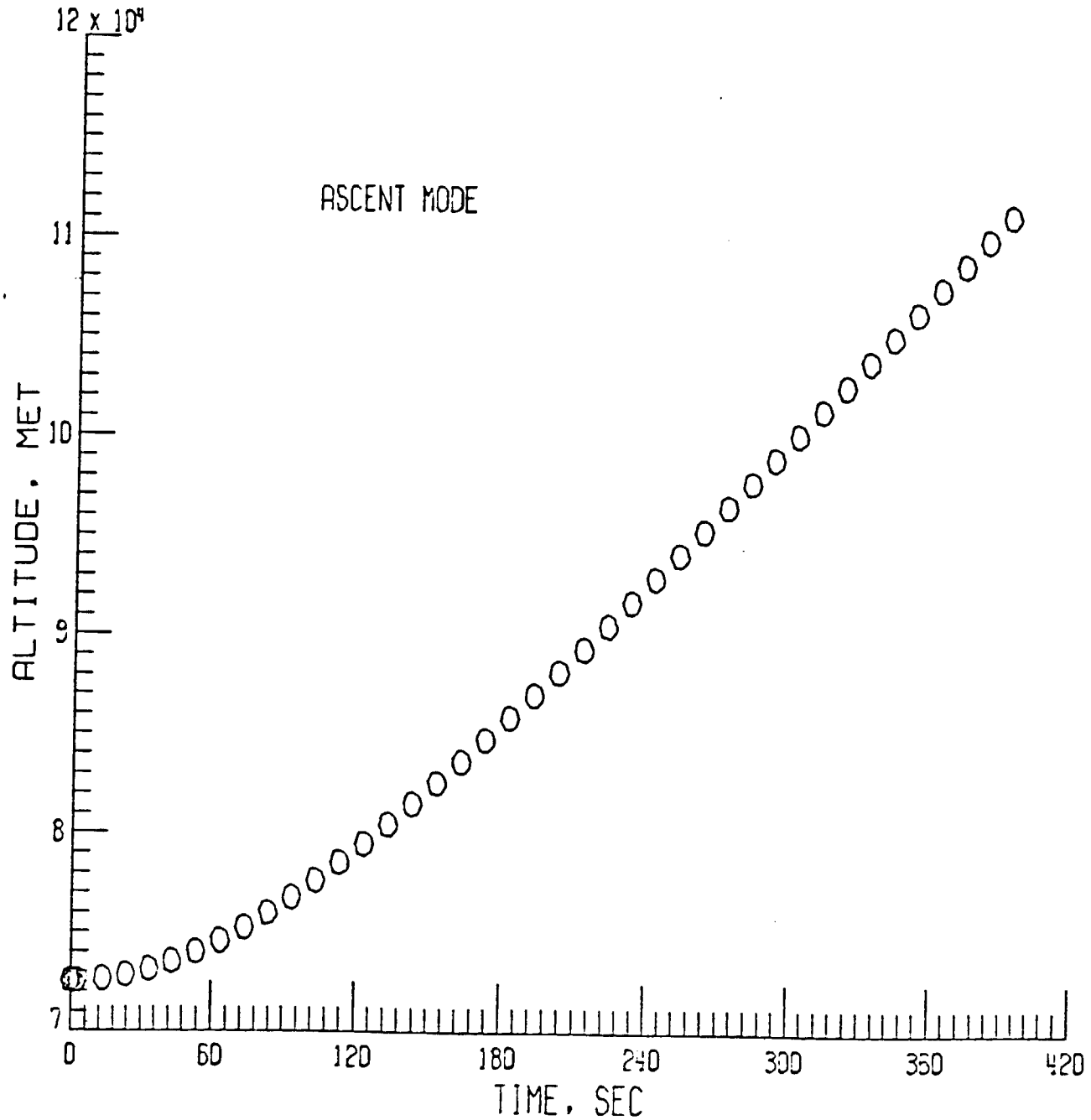


Fig. 14(a). Altitude as a Function of Time During Ascent Mode

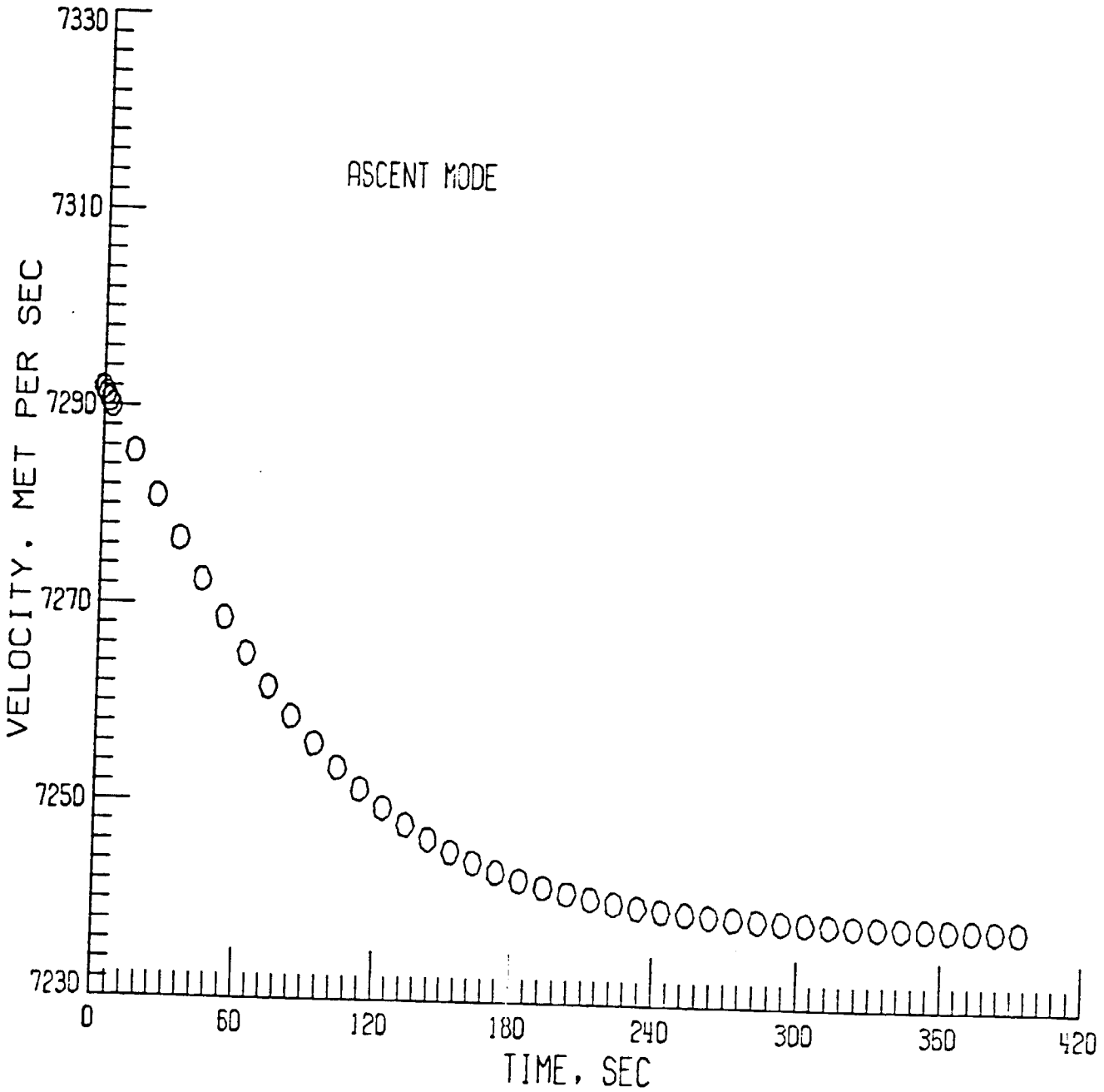


Fig. 14(b). Velocity as a Function of Time During Ascent Mode

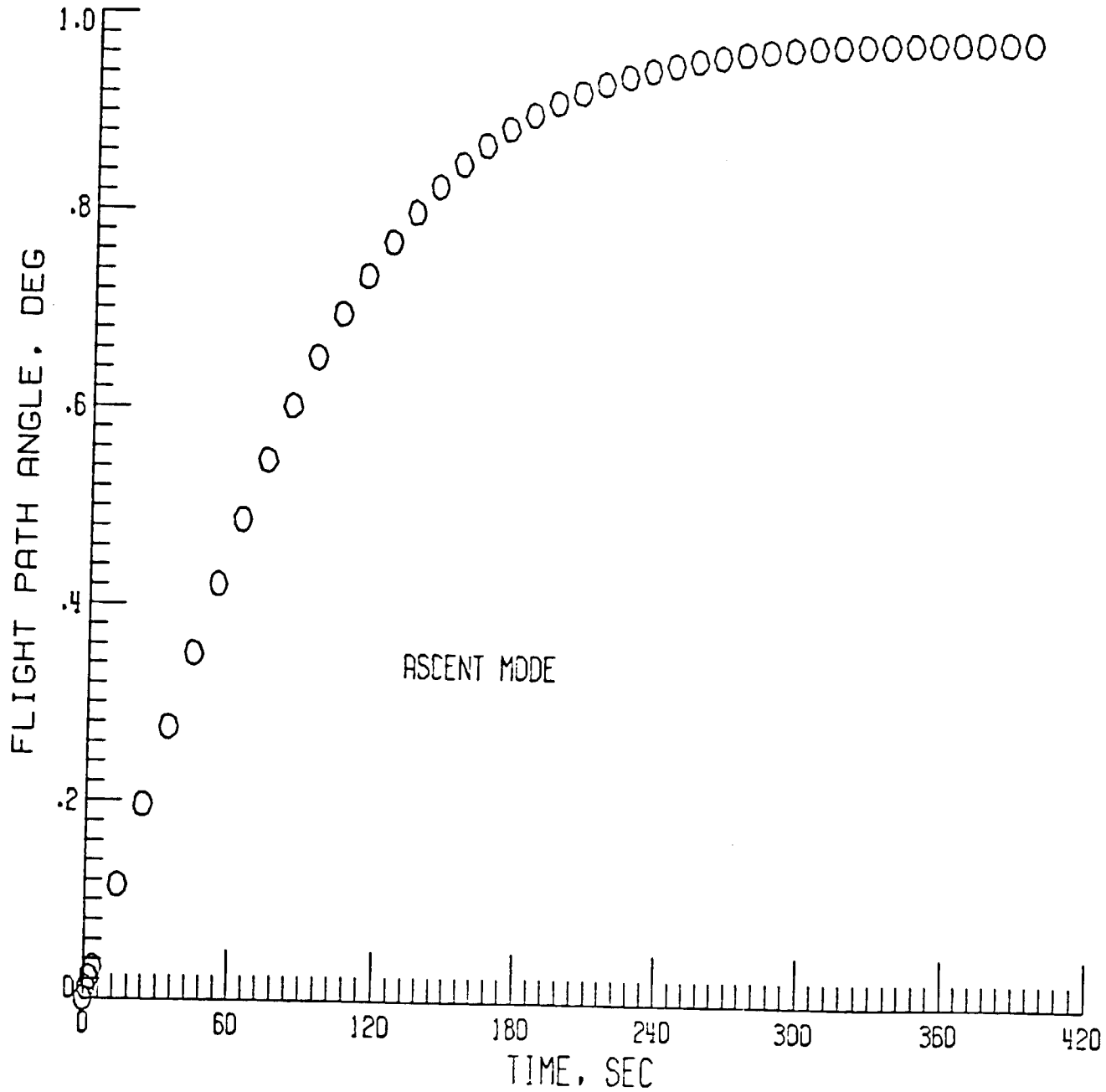


Fig. 14(c). Flight Path Angle as a Function of Time During Ascent Mode

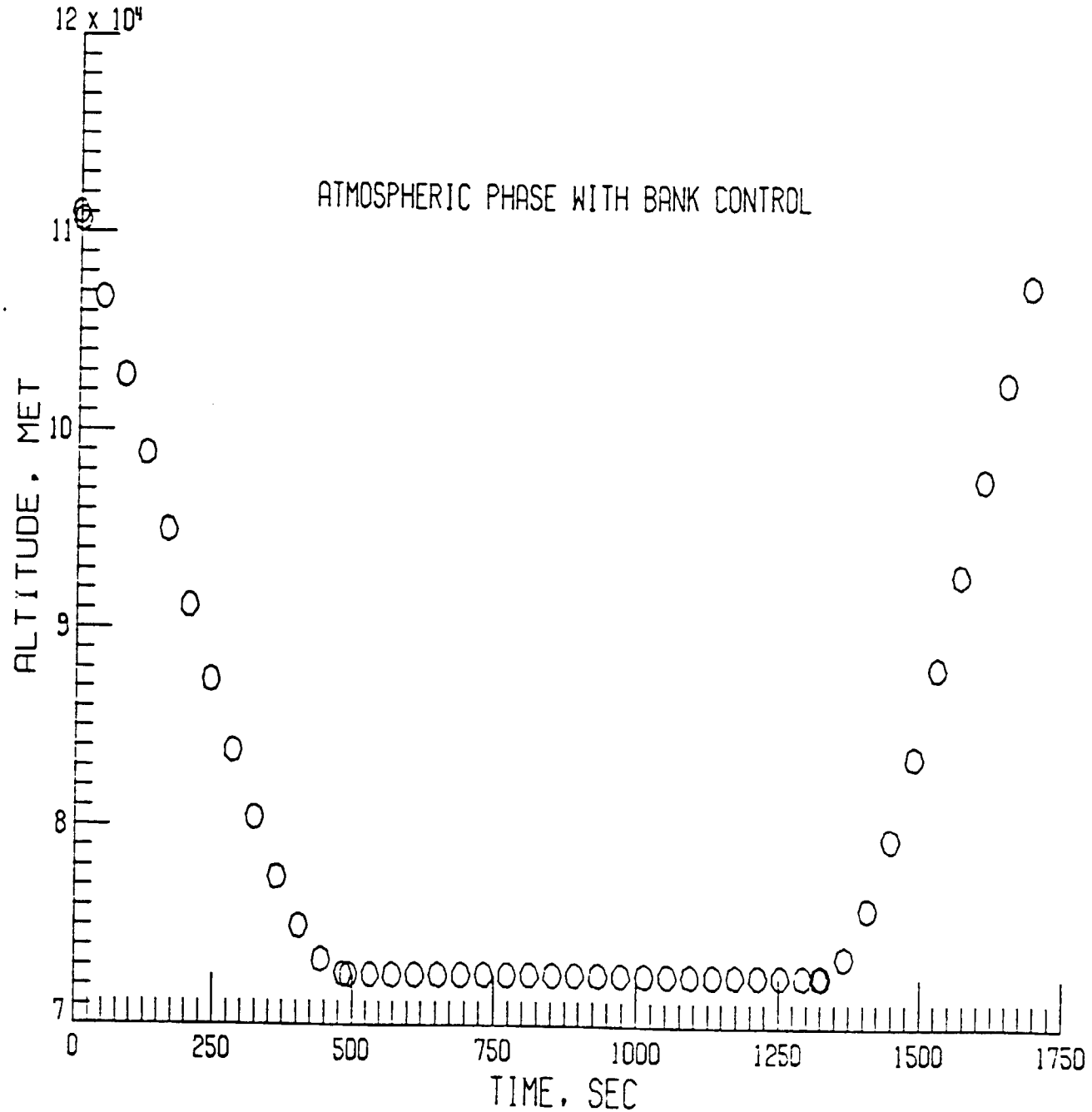


Fig. 15(a). Altitude as a Function of Time with Bank Angle Control

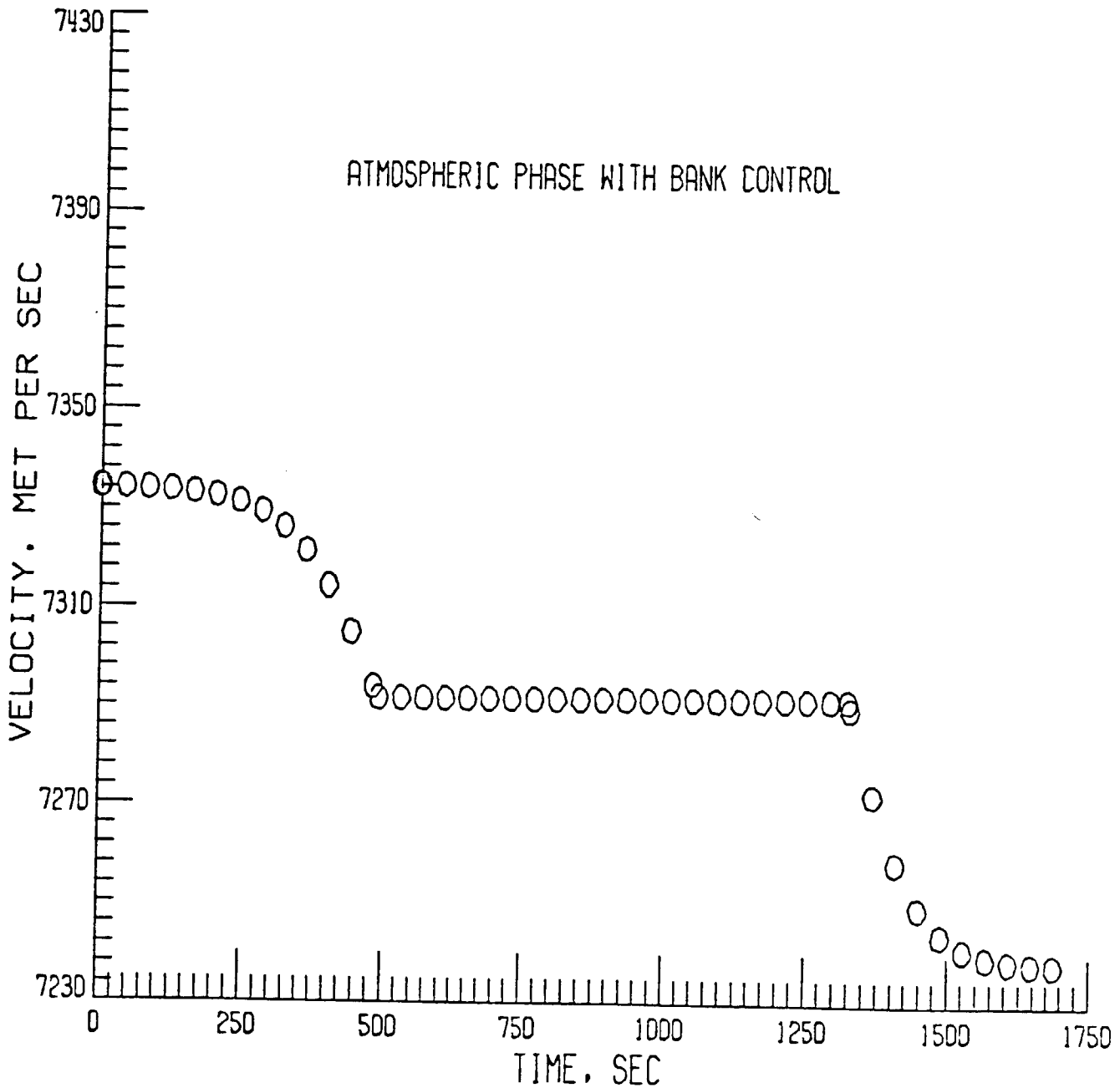


Fig. 15(b). Velocity as a Function of Time with Bank Angle Control

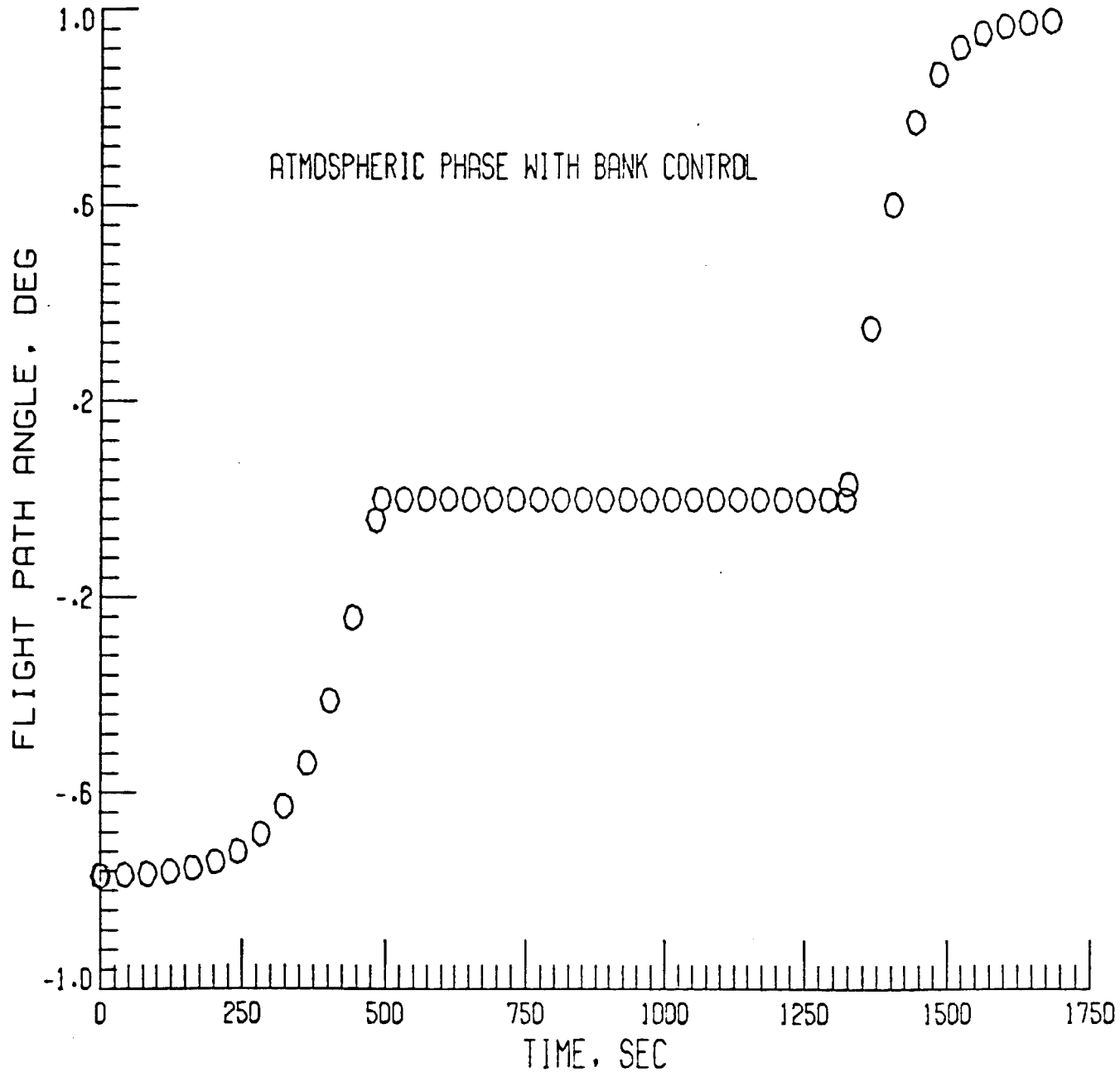


Fig. 15(c). Flight Path Angle as a Function of Time with Bank Angle Control

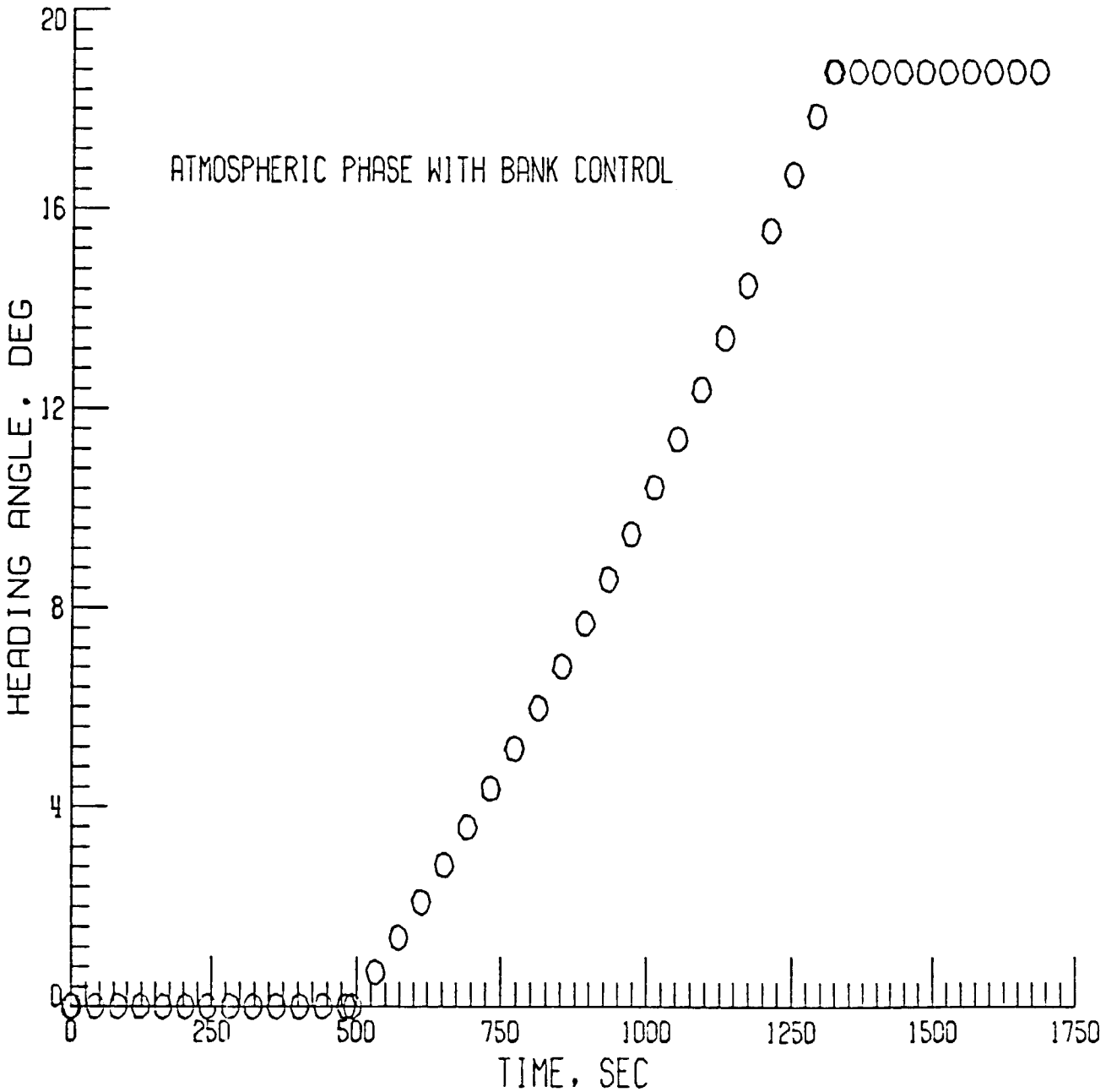


Fig. 15(d). Heading Angle as a Function of Time with Bank Angle Control

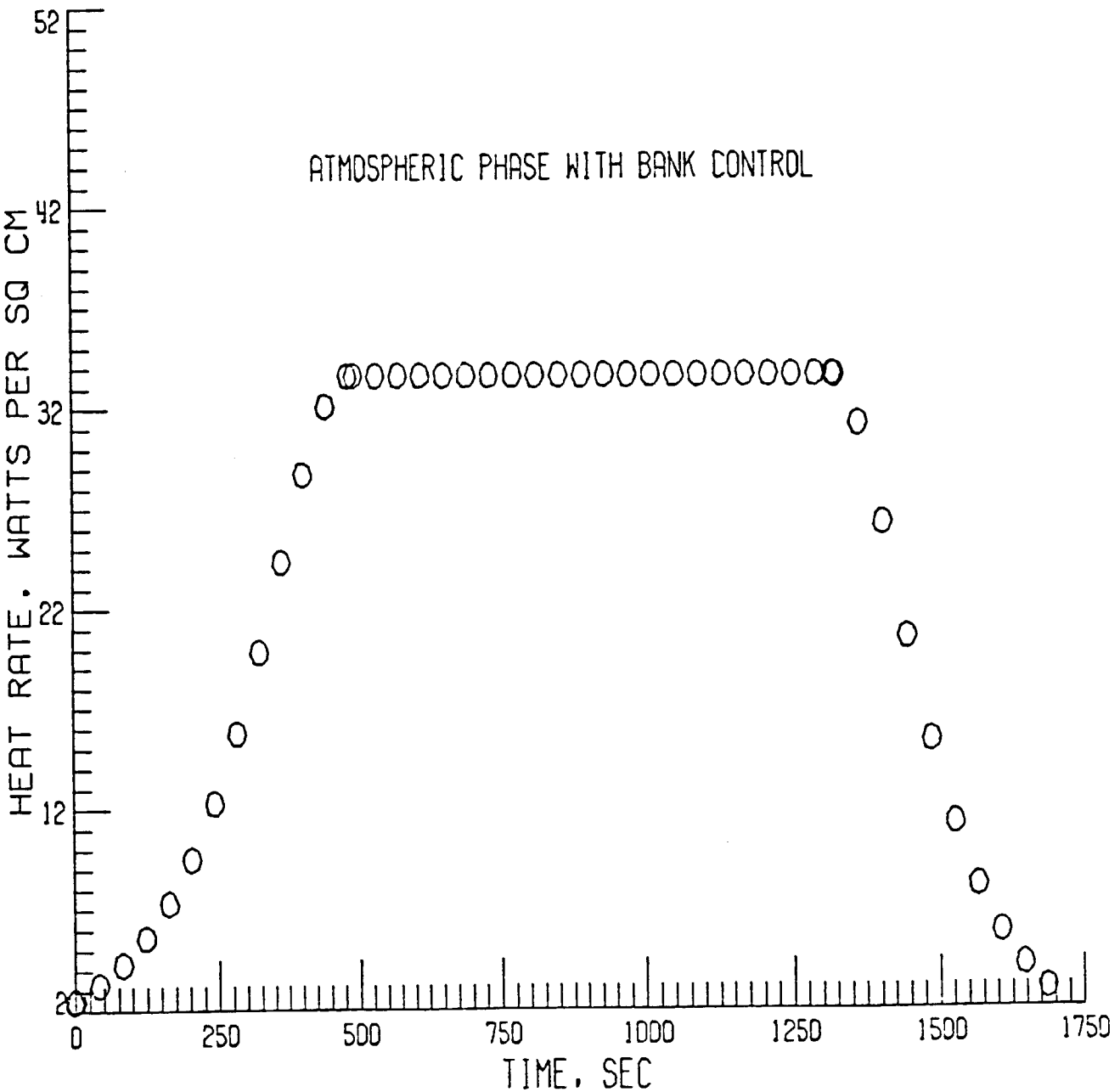


Fig. 15(e). Heat Rate as a Function of Time with Bank Angle Control

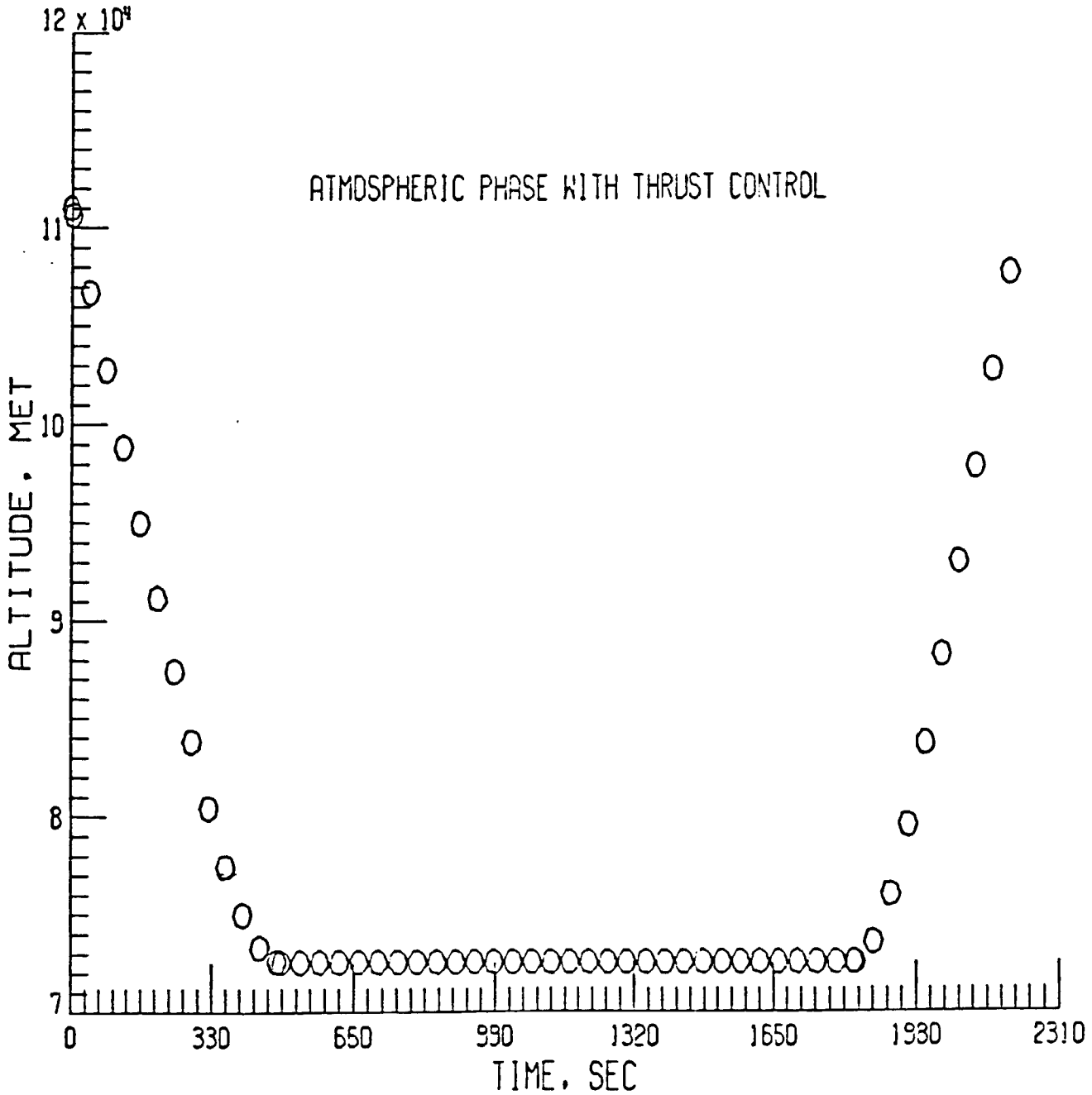
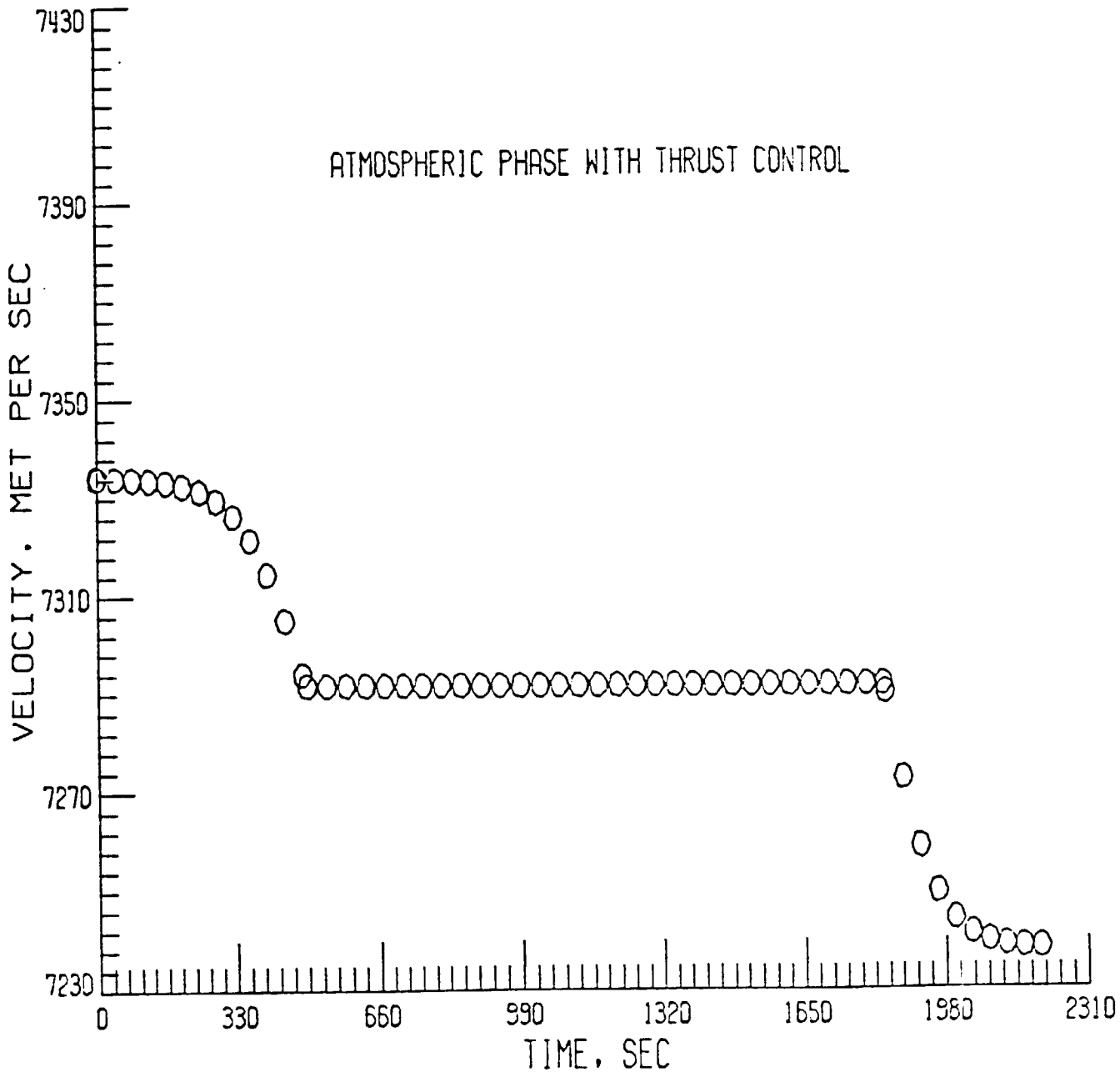


Fig. 16(a). Altitude as a Function of Time with Thrust Control



99

Fig. 16(b). Velocity as a Function of Time with Thrust Control

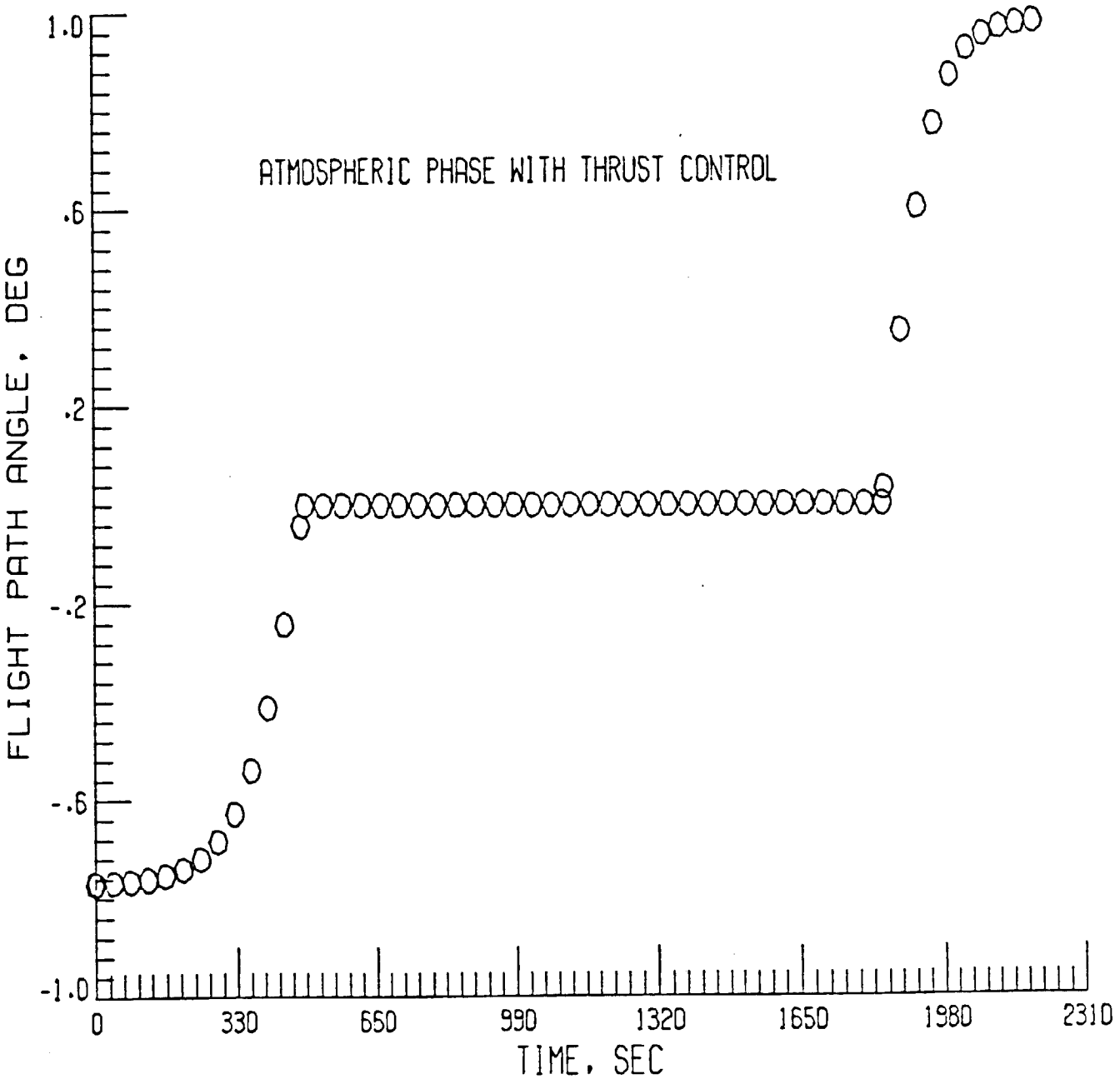


Fig. 16(c). Flight Path Angle as a Function of Time with Thrust Control

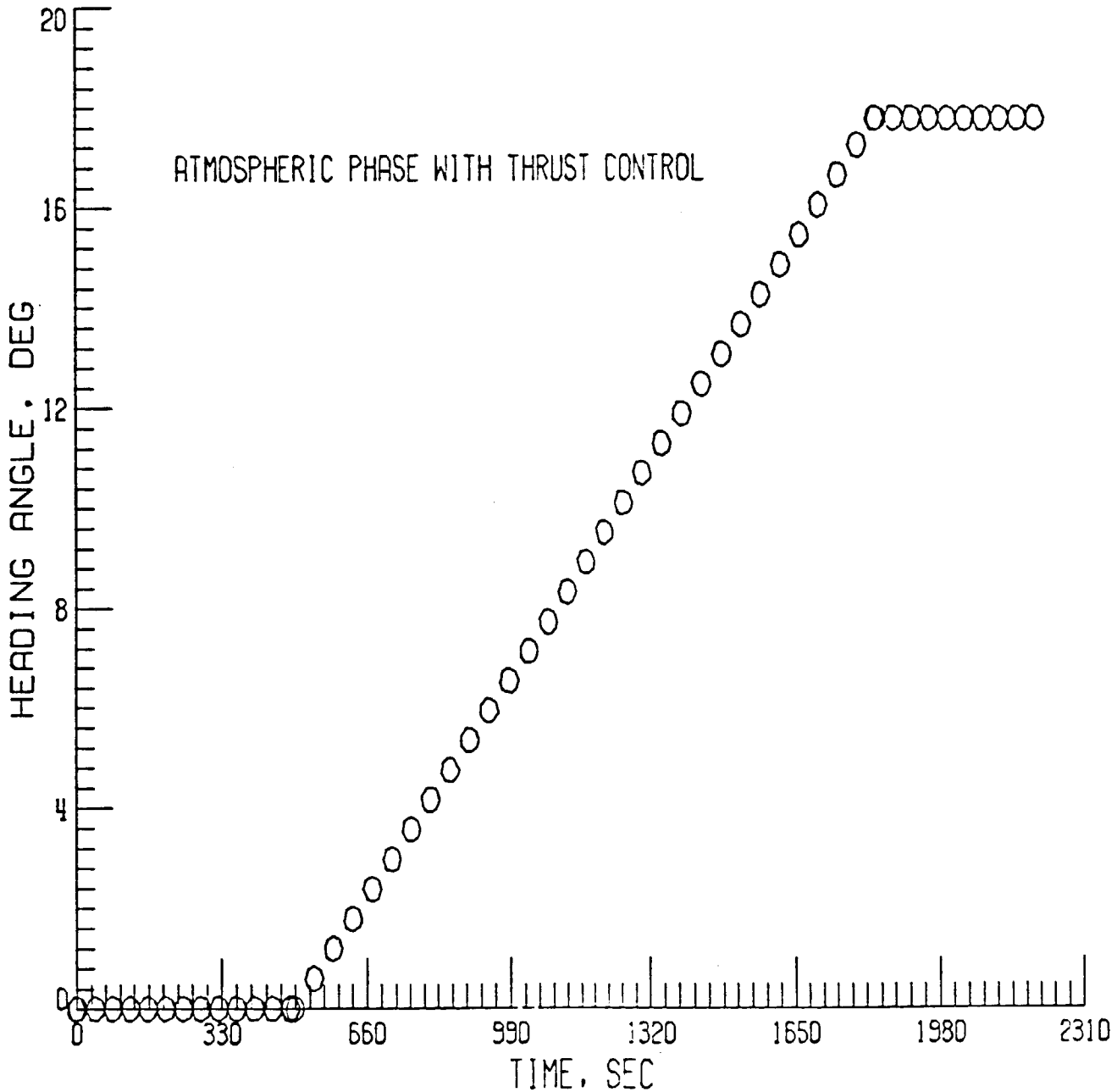


Fig. 16(d). Heading Angle as a Function of Time with Thrust Control

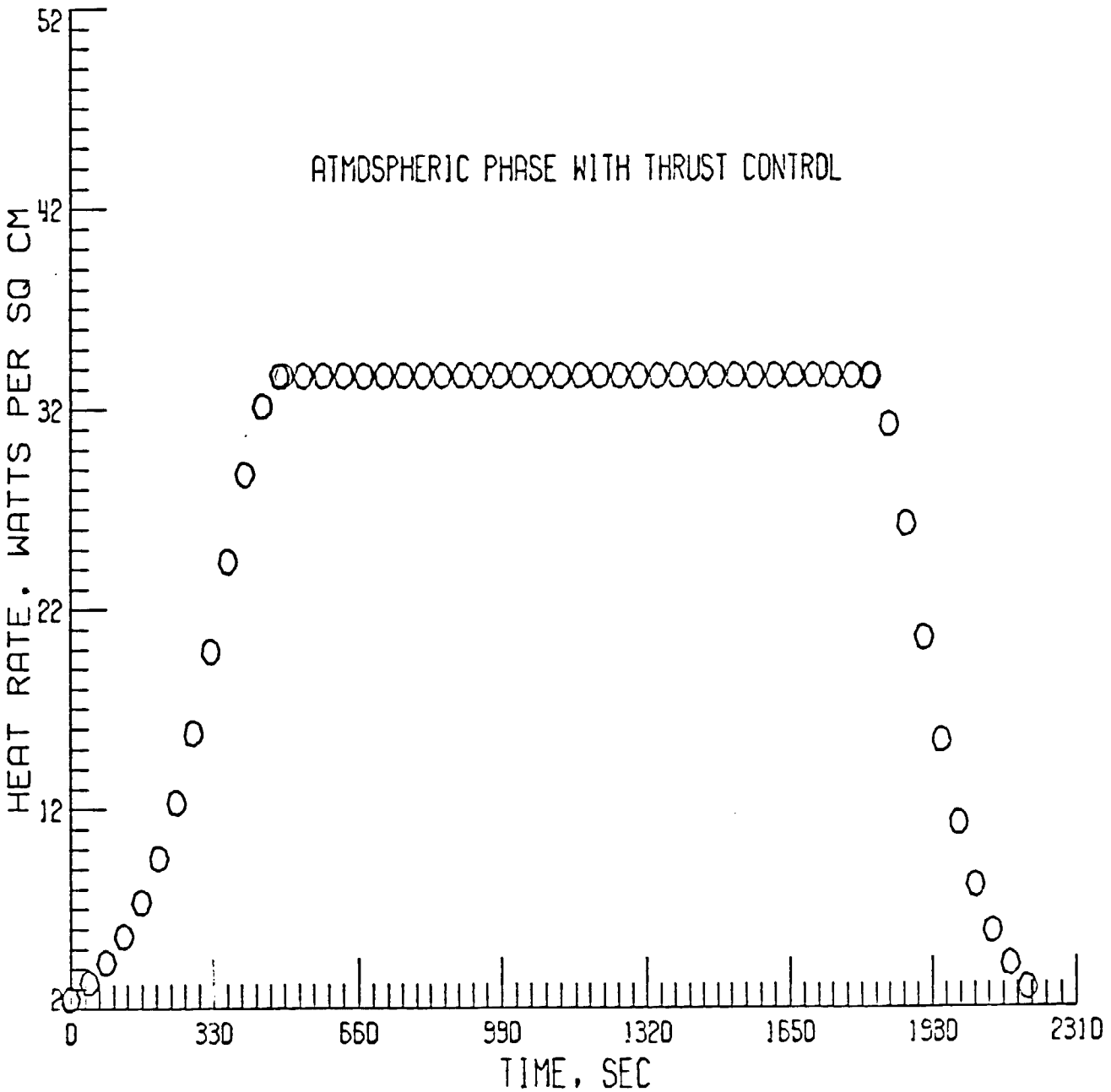


Fig. 16(e). Heat Rate as a Function of Time with Thrust Control